

國立交通大學
光電工程研究所

碩士論文

利用主動層優化降低氮化鎵發光二極體效率下
降特性之研究

Reduction of efficiency droop behavior in InGaN/GaN
light emitting diodes by optimization of active
region

研究生：盧昱昕

指導教授：郭浩中 教授

盧廷昌 教授

中華民國九十九年七月

利用主動層優化降低氮化鎵發光二極體效率下降特性之研究
Reduction of efficiency droop behavior in InGaN/GaN light emitting
diodes by optimization of active regions

研究生: 盧昱昕

Student: Yu-Shin Lu

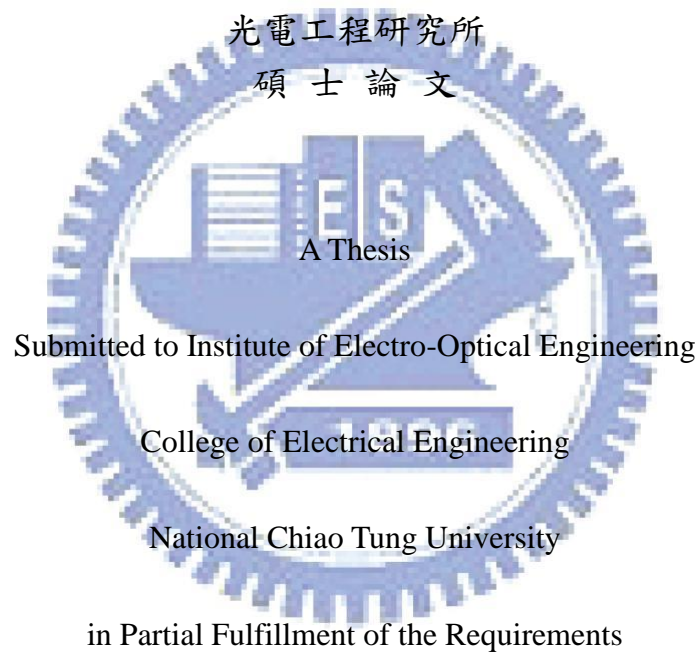
指導教授: 郭浩中 教授

Advisor: Prof. Hao-Chung Kuo

盧廷昌 教授

Prof. Tien-Chang Lu

國立交通大學
光電工程研究所
碩士論文



for the Degree of

Master

In

Electro-Optical Engineering

July 2010

Hsinchu, Taiwan, Republic of China

利用主動層優化改善氮化鎵發光二極體效率下降特性之研究

研究生：盧昱昕

指導教授：郭浩中教授

盧廷昌教授

國立交通大學光電工程研究所碩士班

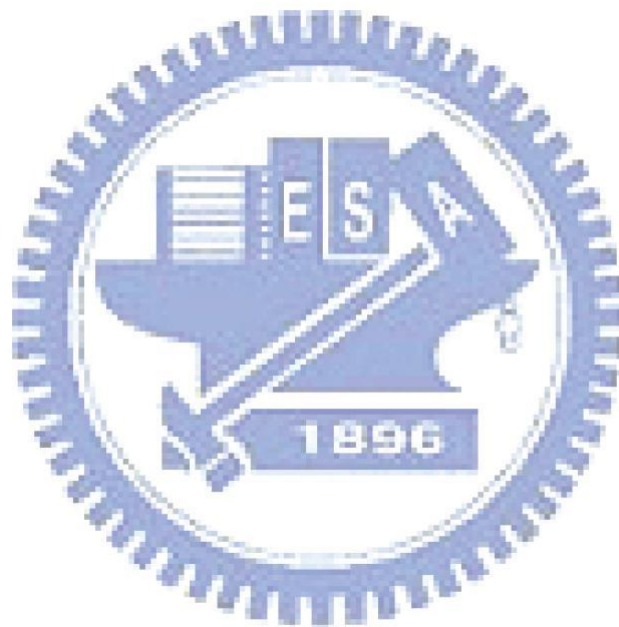
摘要

本論文中，我們利用改善主動層品質及優化量子井結構等方式，試圖提高氮化鎵發光二極體於高電流時的發光效率。我們將低溫成長之氮化鎵薄膜置於n-GaN及主動層間，並將此樣品與一般所使用的InGaN/GaN prestrain layer及未做任何結構之樣品作比較。並更進一步探討在高載子濃度下的LED發光效率，並用漸變式量子井結構進一步改善效率隨載子濃度遞減之情況。我們利用光激發螢光(Photoluminescence, PL)、電激發螢光(Electroluminescence, EL)、以及Advanced Physical Models of Semiconductor Devices (APSYS)模擬軟體等進行樣品的光學與電特性分析。

在本論文中，藉由變強度之光激發螢光實驗我們可以得知有插入prestrain layer之樣品，當載子濃度提高時，其波長藍移量較小，亦即quantum confined Stark effect (QCSE)較小，因此我們可以得知使用低溫成長之氮化鎵薄膜的確是放了主動層內部之應力，並藉由室低溫變強度光激發螢光去定義出三塊樣品之內部量子效率，且有應力釋放之樣品期內部量子效率有明顯提高，並且在高載子濃度時，使用低溫成長之氮化鎵薄膜樣品之效率遞減情況最為輕微，從半高寬與載子濃度的相關圖及CL得表面影像中可以得知低溫成長之氮化鎵薄膜有效降低了主動層內部銻含量分布不均勻之情況，故可以減少載子被非輻射復合中心捕捉之機率

根據以上的實驗結果，使用低溫成長之氮化鎵薄膜及漸變厚度量子井結構的確能有效提升發光二極體之特性。分別在電流密度為 22 A/cm^2 及 244 A/cm^2 時提升效率36%及71%，並且效率遞減的情況從 22 A/cm^2 到 244 A/cm^2 之間效率僅

下降17%.優於傳統結構(54%),



Reduction of efficiency droop behavior in InGaN/GaN light emitting diodes by optimization of active regions

Student : Yu-Hsin Lu

Advisor: Prof. Hao-Chung Kuo

Prof. Tien-Chang Lu

Institute of Electro-Optical Engineering

National Chiao Tung University

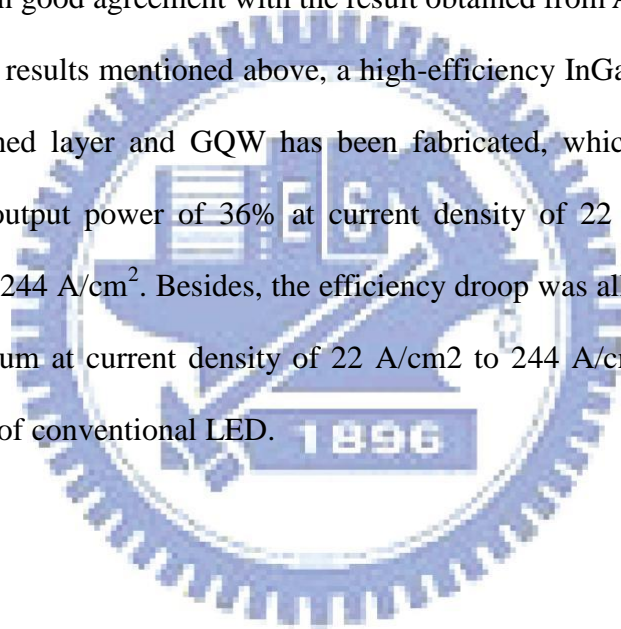
Abstract

Direct wide-bandgap gallium nitride (GaN) and other III-nitride-based semiconductors have attracted much attention for potential applications such as blue, green, and ultraviolet (UV) light-emitting diodes (LEDs) and blue laser diodes (LDs). Although InGaN-based LEDs have many excellent properties, the efficiency droop will occur under high current injection, resulting in the application of lighting was limited. In order to reduce the efficiency droop behavior in InGaN/GaN light emitting diodes, several semiconductor technologies have been used, such as non-polar material, AlInGaN barrier layer, thick DH active region or thick QW, barrier doping etc..

In this study, we tried to reduce the efficiency droop behavior in InGaN-based by using low temperature GaN (LT-GaN) pre-strained layer and graded quantum well (GQW) in which the well-thickness increases along [0001] direction. To better understand the influence of LT-GaN pre-strained layer and GQW on efficiency droop, a lot of measurement techniques were performed to investigate the optical and electrical properties of the grown specimens, including photoluminescence (PL), cathodoluminescence (CL), electroluminescence (EL), L-I-V curve and Advanced Physical Models of Semiconductor Devices (APSYS). From power-dependent PL spectrum, the emission peak wavelength of the specimen with LT-GaN pre-strained

layer and GQW exhibited relatively slight blue shift, which could be related to smaller quantum confined Stark effect (QCSE). Besides, the CL images shown that the specimen has more uniform emission area and less dark spots, resulting in the enhancement in emission efficiency. APSYS simulation analyzed that specimen with LT-GaN pre-strained layer and GQW revealed superior hole distribution as well as radiative recombination distribution. Additionally, according to the analysis of electroluminescence spectrum, specimen with LT-GaN pre-strained layer and GQW reveals additional emission peak from the following narrower wells within GQWs. These results are in good agreement with the result obtained from APSYS simulation.

Based on the results mentioned above, a high-efficiency InGaN-based LED with LT-GaN pre-strained layer and GQW has been fabricated, which demonstrated an improvement in output power of 36% at current density of 22 A/cm^2 and 71% at current density of 244 A/cm^2 . Besides, the efficiency droop was alleviated to be about 17% from maximum at current density of 22 A/cm^2 to 244 A/cm^2 , which is much smaller than 54% of conventional LED.



誌謝

經過兩年的研究生涯，終於要在這階段告一段落了。直到現在，才有一點即將要畢業的感覺。這段日子裡所學到的東西太多了，不僅僅是學術研究上的知識，也包含了為人處事的態度，我要感謝那些在這兩年所有幫助我成長的人。在我遇到問題時不吝幫我解答，使我可以順利的完成我的碩士學位。

首先，我由衷的感謝王興宗老師的指導，老師做學問認真的態度以及爽朗的笑聲深深地影響我；感謝郭浩中老師在我實驗上遭遇困難時，給予我幫助，以及感謝老師平時對我的鼓勵，使我遇到挫折時能更勇敢的面對；感謝盧廷昌老師的指導，使我能夠有許多想法去解決實驗上所遇到的問題。

感謝清華學長，平常Meeting上的指導以及對研究上的規劃和叮嚀，每當我開始怠惰，總是有學長在旁邊鞭策，以及研究上給予的幫助；感謝李博學長，我總是向你詢問許多磊晶及材料上的問題，每次你都不厭其煩的幫助我，也不時會對於實驗上提供不少想法，因為你和清華學長的協助，我才能更順利的完成我的實驗。感謝世邦學長和鏡學學長，有你們的幫助我才能得到穩定的樣品完成研究。感謝小科學長，謝謝你在我碩一時教我熟習實驗的一切架構以及許多LED的基礎知識；感謝Joseph、阿飛、David、dopin、阿翔、依寧、祥淇、永吉、惟雯、哭哭、小胖、小邱、彥群 等碩二的同學，因為你們而讓我的碩士生活更多采多姿，我會永遠記得晚上大家一起跑模擬的日子。感謝瑋婷學妹，謝謝你協助我完成模擬部分的研究，變溫EL實驗有你的冰雪聰明真的輕鬆了許多，感謝祐國學弟，總是很有義氣的陪我們去唱歌。有你們兩個貼心的學弟妹實在很甘心，也祝福你們在未來一年能順利完成你們研究，順利畢業~

感謝所有的學長學弟妹們，每當我一個人在做低溫EL實驗時，總是會有人幫忙買飯和飲料，偶而你們都會來這裡探望一下我，實驗室的笑聲總是會讓我感到很開心，跟著大家一起吃飯聊天總讓我會忘掉實驗上的辛苦。

最後謝謝我的家人，感謝我的爸爸媽媽支持，讓我順利完成學業，謝謝你們。

Content

摘要.....	i
Abstract.....	iii
致謝.....	v
Content.....	vi
List of Tables.....	viii
List of Figures.....	ix

Chapter 1 Introduction

1.1 Wide bandgap III-N materials.....	1
1.2 GaN-based LEDs	2
1.3 Motivation.....	4

Chapter 2 Properties of III-Nitride semiconductor

2.1 Quantum confinement effect in semiconductor nanostructure.....	8
2.2 The electric field and localization effect in quantum well structure.....	9
2.3 The basic concept of inserting prestrain layer.....	11
2.4 The basic concept of efficiency droop.....	11

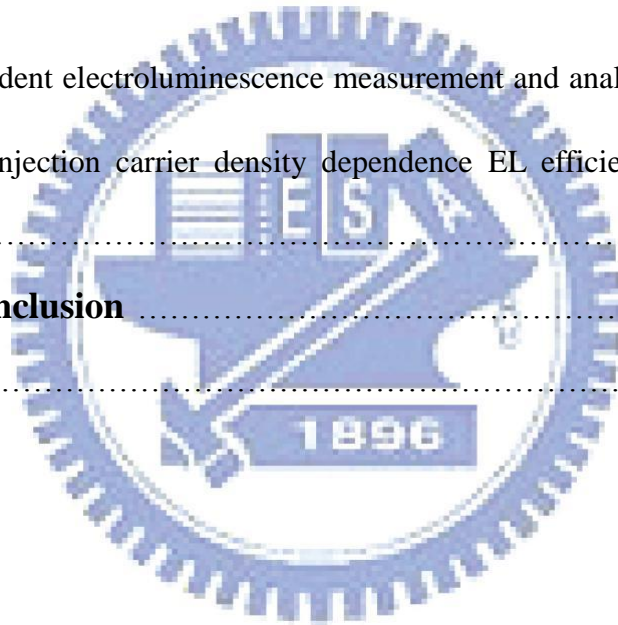
Chapter 3 Experimental instrument and setup

3.1 Photoluminescence (PL)	14
3.2 IQE measurement system.....	16
3.3 Electroluminescence (EL).....	16

Chapter 4 Optical and electrical properties of InGaN/GaN multiple quantum wells with and without prestrain layer

4.1 Introduction.....	20
4.2 Sample structure and Fabrication.....	21
4.3 CL image measurement and discussion.....	22
4.4 Power dependent PL measurement.....	23

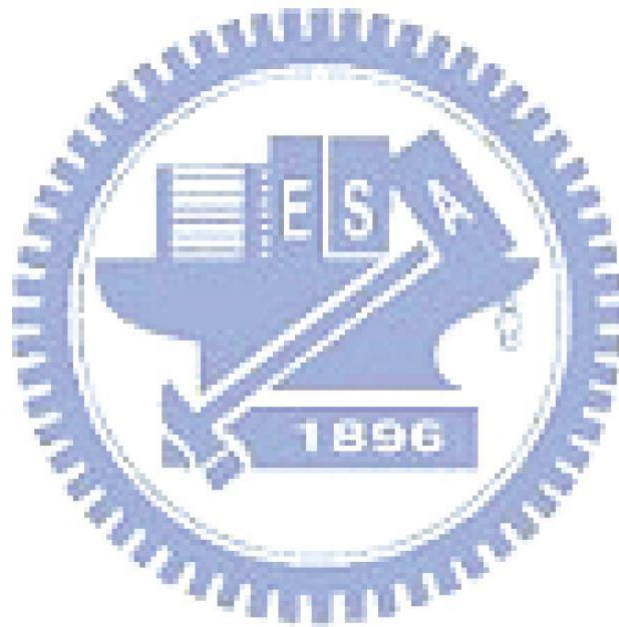
4.5 Temperature dependent PL measurement.....	27
4.6 The measurement of internal quantum efficiency of LED with different prestrain layer.....	28
4.7 Current dependent intensity and efficiency discussion.....	31
Chapter 5 Analysis of electroluminescence and efficiency droop in graded quantum well structure	
5.1 Introduction.....	39
5.2 Sample structure and Fabrication.....	39
5.3 APSYS simulation of electron and hole concentration distribution.....	40
5.4 Current dependent electroluminescence measurement and analysis.....	42
5.5 Analysis of injection carrier density dependence EL efficiency and efficiency Droop.....	44
Chapter 6 Conclusion	53
Reference	55



List of Tables

Table 4.6.1 IQE of InGaN/GaN, LT-GaN and without prestrain layers LEDs.....36

Table 4.7.1 Output power enhance and efficiency decrease.....36



List of Figures

- Figure. 1.1 The bandgap diagram of compound semiconductor materials.
- Figure. 3.1.1. The schematic of experimental Photoluminescence setup.
- Figure. 3.2.1. The schematic of IQE measurement system.
- Figure. 3.3.1. The schematic of EL measurement system.
- Figure. 3.4.1. The picture of electroluminescence system
- Figure. 4.2.1. The schematic drawing of sample structure.
- Figure. 4.2.2. The schematic drawing of fabrication processes of LED.
- Figure. 4.3.1. Top view CL images at corresponding emission peak wavelength.
- Figure. 4.4.1.1 Schematic band diagrams of localized state due to In fluctuation.
- Figure. 4.4.1.2 FWHM of three samples at different carrier density.
- Figure. 4.4.2.1 Emission energy at different power density.
- Figure. 4.5.1. Temperature dependent PL intensity range from 10 to 300 K.
- Figure. 4.6.1. IQE as a function of excitation power at 15K and 300 K.
- Figure. 4.7.1. Emission power as a function of current density of three sample.
- Figure. 4.7.2. Emission efficiency as a function of current density of three sample.
- Figure. 5.2.1. The schematic drawing of sample structure.
- Figure. 5.3.1. Simulated hole distribution in reference and GQW LEDs.
- Figure. 5.3.2. Simulated radiative recombination distribution

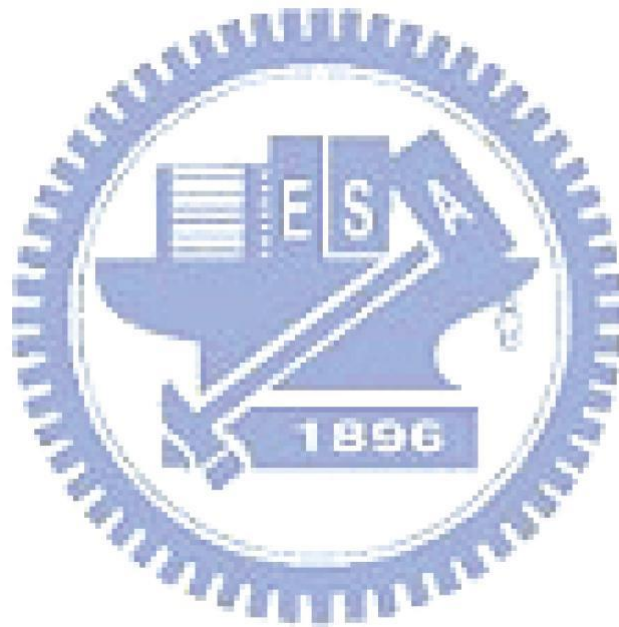
Figure. 4.1 Current-dependent electroluminescence spectra .

Figure. 5.4.2. Current-dependent asymmetry factor of electroluminescence spectra .

Figure. 5.4.3. Current dependent emission energy and FWHM.

Figure. 5.5.1. Comparison of electroluminescence efficiency and L-I curves.

Figure. 5.5.2. APSYS simulation electroluminescence efficiency and L-I curves.



Chapter 1 Introduction

1-1 Wide bandgap III-N materials

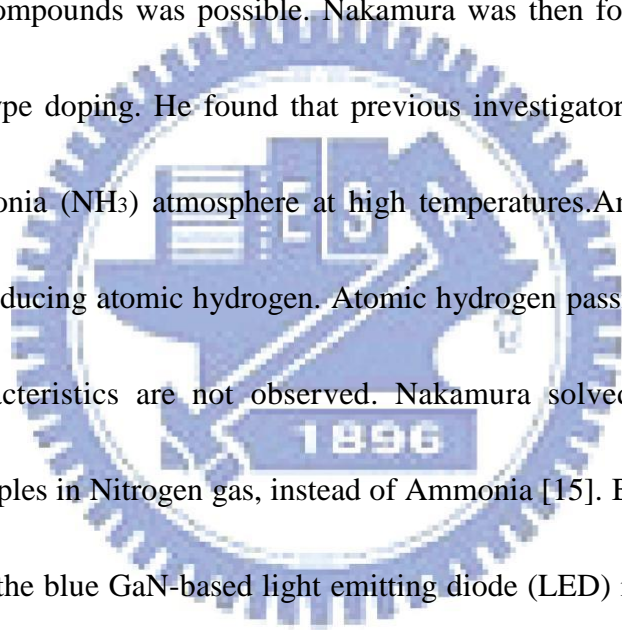
Wide bandgap nitride materials have attracted great attention over the past decades. The bandgap of the III-nitrides like AlN, GaN and InN material cover a very wide range from 0.9 to 6.1 eV which represents the emission wavelength from deep ultraviolet (UV) to infrared (IR) region as shown in Figure 1.1. This wide emission wavelength range makes it promising for applying in the applications of optoelectronic devices such as flat panel display, competing storage technologies, automobiles, general lighting and biotechnology, and so on [1-4]. It is worth noting that as the rapid developing of the blue region material research, we are able to fill up the visible light gap and make the full color display by semiconductor material becomes possible. Besides, the emitted short wavelength light in the blue and UV region is especially suitable to pump up the yellow light and comes out a white light output by mixing the original blue source and excited yellow light which realized the solid state lighting. The III-nitride semiconductor material enjoyed some unique properties that not only suitable for lighting source in short wavelength in visible region but also high-speed/high-power electron device [5]. For example, it has high bond energy (~ 2.3 eV), high-saturation velocity ($\sim 2.7 \times 10^4$ cm/s), high-breakdown field ($\sim 2 \times 10^6$ V/cm), and strong excitonic effects (>50 meV) [6-7]. However,

considered as a next generation high efficiency lighting devices, III-nitride semiconductors have some inherent drawbacks to deteriorate the lighting efficiency like internal piezoelectric field and spontaneous polarization at heterointerface leading to the quantum confined Stark effect (QCSE) and causing charge separation between electrons and holes in quantum wells [8-9]. Even though, it is still worth to devote more effort to overcome such problems for its great potential for realization of next generation solid state lighting.

1-2 GaN-based LEDs

Basically, the blue GaN-based LED confronts some severe problems lowering the efficiency and hindering the realization of solid state lighting. Lack of suitable substrate GaN epitaxy is the most important issue. Nowadays, GaN material was grown on sapphire substrate, which has a 15% smaller lattice constant than GaN, and different thermal expansion coefficient. That leads to a very high defect density and cracking of the layers when the structures are cooled down after growth. The problem was firstly solved by Amano and Akasaki by designing and growing a AlN buffer layer in 1986 [10]. Also, Nakamura grew GaAlN buffer layers on top of sapphire in 1991 [11] which make it possible to grow GaN on sapphire. In addition to the invention of buffer layer, Prof. S. Nakamura also solved the high growth temperature

problems by his two-flow growth reactor which opens the door of high quality GaN material on sapphire [12]. The third problem of for GaN-based LED is p-type doping. Every semiconductor lighting device needs p-n junctions. Previous to Akasaki's work p-type doping of GaN was impossible. Akasaki (1988 at Nagoya University) found that samples after Low Energy Electron Beam Irradiation treatment (LEEBI) showed p-type conductivity [13-14]. Thus Akasaki demonstrated that in principle p-type doping of GaN compounds was possible. Nakamura was then found the solution to the puzzle of p-type doping. He found that previous investigators had annealed the samples in Ammonia (NH_3) atmosphere at high temperatures. Ammonia dissociates above 400°C , producing atomic hydrogen. Atomic hydrogen passivates acceptors, so that p-type characteristics are not observed. Nakamura solved this problem by annealing the samples in Nitrogen gas, instead of Ammonia [15].



Benefit by the effort of such pioneers, the blue GaN-based light emitting diode (LED) is now successfully commercialized. The typical structure of a blue GaN-based LED is illustrated in Figure 1.2. The layer of n-type GaN contains an excess of electrons, whereas the p-type layer is a region from which electrons have been removed (i.e., in which “holes” have been formed). If a forward bias is applied, electrons and holes can recombine, releasing energy in the transition layer in the form of light. The energy of the photon corresponds to the voltage bias in the transition region (the “bandgap”).

Sapphire and silicon carbide are often used as substrates, which allow for large-area heteroepitaxial growth.

1-3 Motivation

Typical InGaN/GaN LED are characterized by a substantial decrease in efficiency as injection current increases. This phenomenon which known as efficiency droop is a severe limitation for high power devices that operate at high current densities and must be overcome to enable the LEDs needed for solid-state general illumination. The efficiency droop is caused by a nonradiative carrier loss mechanism, which is small at low currents but becomes significant for high injection currents. Competition between radiative recombination and this droop-causing mechanism results in the reduction in efficiency as current increases. The physical origin of efficiency droop remains controversial, and several different mechanisms have been suggested as explanations, including carrier leakage from the active region [16]. Auger recombination [17], junction heating [18], and carrier delocalization from In-rich low-defect-density regions at high carrier densities [19]. Carrier leakage in GaInN LEDs generally refers to the escape of electrons from the active region to the p-type region. These leakage electrons may then recombine with holes either in the p-type region or at the contacts, dominantly by nonradiative processes. Necessarily,

therefore, fewer holes than electrons are injected into the active region. These two phenomena that escape of electrons from the active region and reduced hole concentration of any carrier leakage explanation for droop. Hole injected into the active region may be the limiting factor, possibly due to the low p-type doping efficiency or the electron blocking layer (EBL) acting as a potential barrier also for holes. As a result of the low hole injection, current across the device is dominated by electrons. Devices with p-type active regions which should increase hole injection efficiency have been proposed as a solution to this problem.

However, it is not clear which cause the efficiency droops at high current. For this study, we investigated the excitation power dependence PL intensity at room temperature and temperature dependent intensity to confirm the confinement of carrier in different structure. Then we discussed the normalized efficiency as a function of injection current density at room temperature clearly and used APSYS simulation to make sure our model is correct, so the physical mechanisms of current dependent efficiency of InGaN/GaN LED has been confirmed.

This thesis is organized in the following way: In chapter 2, we give some theoretical backgrounds and characteristics about InGaN/GaN MQW structures. The experimental setups and theory are stated in chapter 3. In chapter 4, we present the experiment results and discuss for optical and electrical properties of InGaN/GaN

MQW LED with LT-GaN, InGaN/GaN and without prestrain layer. In chapter 5, we show the experiment results and discuss for physical mechanisms of graded quantum wells as a function of injection current density in InGaN/GaN LEDs. Finally, we gave a brief summary of the study in chapter 6.

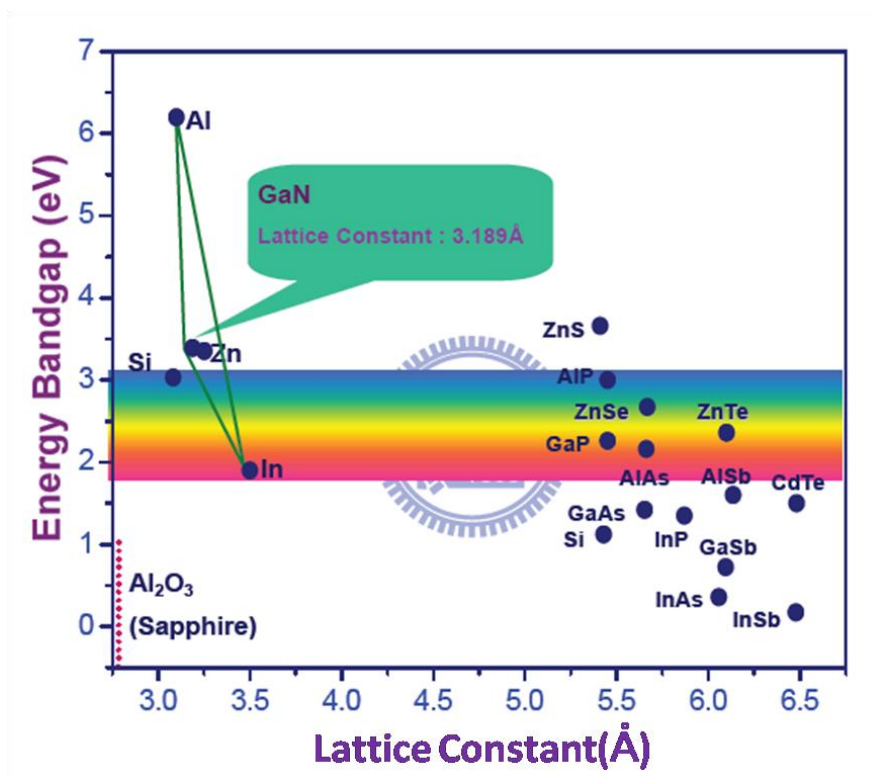


Figure 1.1 The bandgap diagram of compound semiconductor materials.

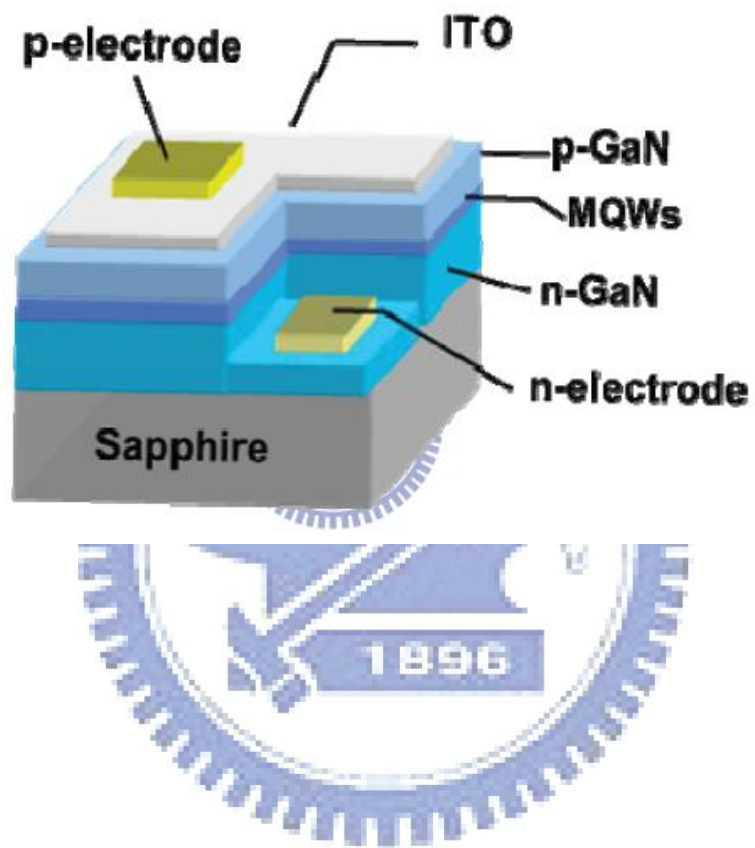


Figure 1.2 The schematic of typical p-side up GaN-based LED

Chapter 2 Properties of III-Nitride semiconductor

In this chapter, we show the properties of InGaN/GaN LEDs and prestrain insertion layer in InGaN/GaN light emitting diodes. Efficiency droop behavior has also be introduced

2-1 Quantum confinement effect in semiconductor nanostructure

The semiconductor nanostructure is widely used as the active layer in optoelectric devices such as light emitting diodes and laser diodes. This low dimension structure has the advantage of high emission efficiency because of the quantum confinement effect. Due to the different dimension of confinement, we can divide the nanostructures into several groups. For instance, the quantum well structure is confined in one dimension (1D), the quantum wire structure is confined in two dimensions (2D), and the quantum dot structure is confined in three dimensions (3D). In this thesis, we would discuss the quantum well structure in detail.

When we discuss the quantum well structure, the excitons are confined in two dimensions. If the well width is much larger than a_B in bulk, the exciton would not feel any difference compared to the environment in bulk. However, if the well width decreases to the order of a_B in bulk or even smaller than a_B in bulk, the electrons and holes would be strongly confined in the well and also increase the exciton binding energy.

With above discussion, the Hamiltonian of the relative motion can be written as

$$H=H_e(x_e, y_e, z_e) + H_h(x_h, y_h, z_h) + H_{e-h}(r) \quad \text{Eq. (2.1.1)}$$

where H_e and H_h are represented as the electron and hole motion confined in the well, and H_{e-h} is the Hamiltonian described the Coulomb potential attracting the electron and hole in the three dimension confinement. The x - y - z coordinate is defined due to

different spatial confinement and r is the relative position vector between the electrons and holes. Therefore, the resolution of the Hamiltonian is given by

$$E_n = E_{n+}^e + E_n^h - E_{e-h} \quad \text{Eq. (2.1.2)}$$

where E_n^e and E_n^h is the energy of n^{th} quantum confined state, and E_{e-h} is the binding energy of exciton. Then, the lowest exciton resonance energy associated with the ground states in the well can be described as

$$E_{res} = E_g + E_{n+}^e + E_n^h - E_{e-h} \quad \text{Eq. (2.1.3)}$$

In actual situation, the exciton resonance energy is sensitive to the well width. When we use narrow well width, the confinement is improved. However, when the well width is extremely narrow, there may be some leakage of the electron and hole wave function leading to the decreasing of the exciton binding energy. The emission spectrum of the quantum well structure is affected by the competition between the quantum confinement energy level and that of exciton binding energy.

2-2 The electric field and localization effect in quantum well structure

In consequence of the polar crystal structure group III-nitride heterointerfaces are charged [20, 21]. Strong electric fields therefore influence valence and conduction band profiles at interfaces [21] and in quantum wells [22–25]. Any deformation of the gallium nitride lattice modifies the interatomic distances as well as the polarisation of the unit cell and occur in correlation with changes of interface charges and of the band structure [26–28]. Therefore, precise knowledge of the strain evolution in epitaxial

gallium nitride layers preceding the growth of the actual device structure is of high interest. The built-in electric field in conventional *c*-plane heterostructures would result in decreasing the oscillation strength of the separation of electron-hole pairs. Also, the carrier recombination rate and the internal quantum efficiency would be reduced.

However, in spite of the high density of dislocations and large separation of electron-hole pairs, the InGaN-based heterostructures grown on *c*-plane sapphire still have the high luminescence efficiency. It is reported that the luminescence efficiency enhancement is due to the effective localization of excitons in the In-rich regions [29]. The mechanism of this unique behavior in InGaN-based heterostructures is still unclear. Several groups suggested that the localization of excitons might induce by the composition fluctuation and the phase separation [30,31]. In the In-rich regions, it would provide a deep potential minimum within the InGaN layers, which would confine electrons and holes tightly. Once the carriers injected into the InGaN-based heterostructures, they will not be captured by the defects or dislocations. The effectively trapping of carriers improved the radiative recombination rate.

Otherwise, the exciton localization is influenced by quantum well thickness, In content, and doping level. The increase of In content may increase the effective localization depth but also induce more nonradiative defect densities [32].

2-3 The basic concept of inserting prestrain layer

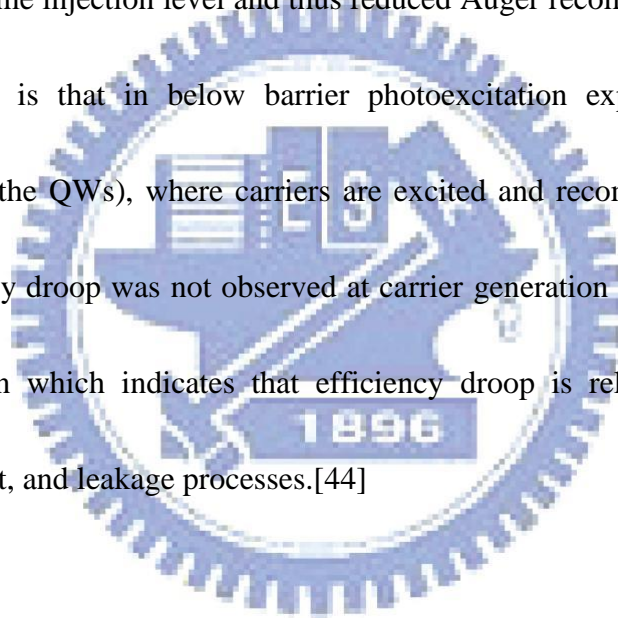
In general, the light output for a multiple quantum well (MQW) light-emitting diode (LED) depends on the internal quantum efficiency (IQE) and the light extraction efficiency (LEE). The former case mainly depends on the quality of materials and their heterointerfaces within the active region. In addition, the quality of the layer interfaces below and above the active region would also affect LED performance. For GaN-based LEDs, the influence of magnesium or silicon dopants in InGaN/GaN MQW on the IQE of GaN-based LEDs has been reported in previous studies. Their performances could be also improved by the insertion of a prestrain layer(s) between the InGaN/GaN MQW and the n-GaN [33]. It has been proposed that the high luminescence efficiency results from successfully reducing compress strain and enhancing quality in active regions. However, the In fluctuation in the InGaN layers may also induce more nonradiative defect densities and influence efficiency at high carrier density.

2-4 The basic concept of efficiency droop

Solid-state lightings, especially InGaN/GaN light-emitting diodes (LEDs), have been vigorously developed to take the place of traditional lighting source, due to its potentially higher efficiency. It is imperative that LEDs produce high luminous flux

which necessitates high efficiency at high current densities. However, as the efficiency of LEDs increases, the upcoming challenge is the efficiency “droop” for high-power applications [34]. The external quantum efficiency EQE reaches its peak at current densities as low as 50 A/cm² and monotonically decreases with further increase in current.[35] It means that the efficiency reduces rapidly when LED operating under high carrier density. Contrary to what may appear at an instant glance, dislocations have been shown to reduce the overall efficiency but not affect the efficiency droop. The major cause of efficiency droop is still a huge controversy. Various possible mechanisms of droop including carrier overflow [35], non-uniform distribution of holes [36, 37], Auger scattering [38], carrier delocalization [39], junction heating have been proposed, but the genesis of the efficiency droop is still the topic of an active debate. Although Auger recombination was proposed for the efficiency droop,[40]the Auger losses in such a wide bandgap semiconductor are expected to be very small,[41] which has also been verified using fully microscopic many body models.[42] In addition, if an inherent process such as Auger recombination were solely responsible for the efficiency degradation, this would have undoubtedly prevented laser action, which requires high injection levels, in InGaN which is not the case. The efficiency droop was also noted to be related to the quantum well thickness in the form of peak efficiency shifting to higher injection currents with

increasing well thickness.[43] It was suggested that the effect of polarization field may be playing a role.[44] The observations, however, are consistent with large effective mass of holes because of which it is very likely that only the first QW next to the p -barrier substantially contributes to radiative recombination. Making the well wider, therefore, increases the emission intensity providing that the layer quality can be maintained. It has also been suggested that in wider QWs the carrier density is reduced for the same injection level and thus reduced Auger recombination.[44] What is very revealing is that in below barrier photoexcitation experiments (photons absorbed only in the QWs), where carriers are excited and recombined in the QWs only, the efficiency droop was not observed at carrier generation rates comparable to electrical injection which indicates that efficiency droop is related to the carrier injection, transport, and leakage processes.[44]



Chapter 3 Experimental instrument and setup

3-1 Photoluminescence (PL)

PL spectroscopy has been used as a measurement method to detect the optical properties of the materials because of its nondestructive characteristics. PL is the emission of light from a material under optical excitation. The laser light source used to excite carriers should have larger energy band gap than the semiconductors. When the laser light is absorbed within the semiconductors, it would excite the carriers from the valence band to the conduction band. Then, it produces the electrons in the conduction band and the holes in the valence band. When the electron in an excited state return to the initial state, it will emit a photon whose energy is equal to the energy difference between the excited state and the initial state, therefore, we can observed the emission peak from PL spectrum.

The photoluminescence spectroscopy is the optical measurement to examine the quality and optical characteristic of material. First, when we analysis a new compound semiconductor, we can use PL measurement to know the band gap of the new material. Second, the intensity of PL signal is contributed to the amount of radiative recombination in the materials. Therefore, PL measurement can be used to understand

the material quality and the recombination mechanisms of the materials.

The carrier recombination processes occur in many ways in order to reach the equilibrium. Those processes can be divided into radiative recombination and nonradiative recombination. We can recognize the radiative recombination easily at low temperature by PL measurement, since it would not be influenced by the thermal energy.

If there are some defect energy level existed in energy band gap of semiconductor, they could also contribute to radiative recombination process. Therefore, we could observe the multiple emission peaks in the PL spectrum, and the intensity of the emission peaks is related to the contribution of the individual radiative recombination process.

The schematic setup of our PL system is shown in Fig. 3.1.1. The pumping source was a multi-mode and non-polarized Helium-Cadmium laser operated on 325 nm with 35 mW. After reflecting by three mirrors, the laser light was focused by a lens which focal length was 5 cm, to 0.1 mm in diameter and the luminescence signal was collected by some lens. The probed light was dispersed by 0.32 monochromator (Jobin-Yvon Triax-320) with 1800, 1200, and 300 grooves/mm grating and the maximum width of the entrance slit was 1 mm. In order to prevent the laser coupling with the PL spectrum, we used the long pass filter in front of the entrance slit. In the

temperature-dependent PL measurement, all the samples were placed in the closed-cycle cryostat with a temperature controller ranging from 20 K to 300 K.

3-2 IQE measurement system

The schematic setup of our IQE measurement system is shown in Fig. 3.2.1. The pulsed excitation source for the IQE measurement is provided by the frequency doubler (2ω) or frequency tripler (3ω) beams of a mode-locked Ti: sapphire laser (ω) which was pumped by Ar^+ laser. The wavelength of Ti: sapphire laser is tunable from 700 nm to 900 nm and the pulse width is 200 fs. The repetition rate of the Ti: sapphire laser is 76 MHz whose time interval is 12.5 ns. The PL luminescence spectrum was measured in conjunction with monochromator using gratings whose grooves are 2400 lines/grooves. To directly examine the optical properties of InGaN/GaN MQW LEDs and avoid the absorption of GaN film, the pumping light source was a frequency doubled Ti: sapphire laser operated on 390 nm. And all the samples were placed in the closed-cycle cryostat with a temperature controller ranging from 20 K to room temperature.

3-3 Electroluminescence (EL)

Fig. 3.3.1 shows the schematic of low electroluminescence measurement systems. A set of instruments including current source Keithley 238, a microscope to observe

the patterned electrode of sample surface, three axial stages for probe and fiber to detected the light output, and a cryostat for the cooling system which use the liquid helium to cooling the chamber. Then, the light detected by a 0.32 m monochromator (Jobin-Yvon Triax-320) with 1800, 1200, and 300 grooves/mm grating and the maximum width if the entrance slit was 1 mm.

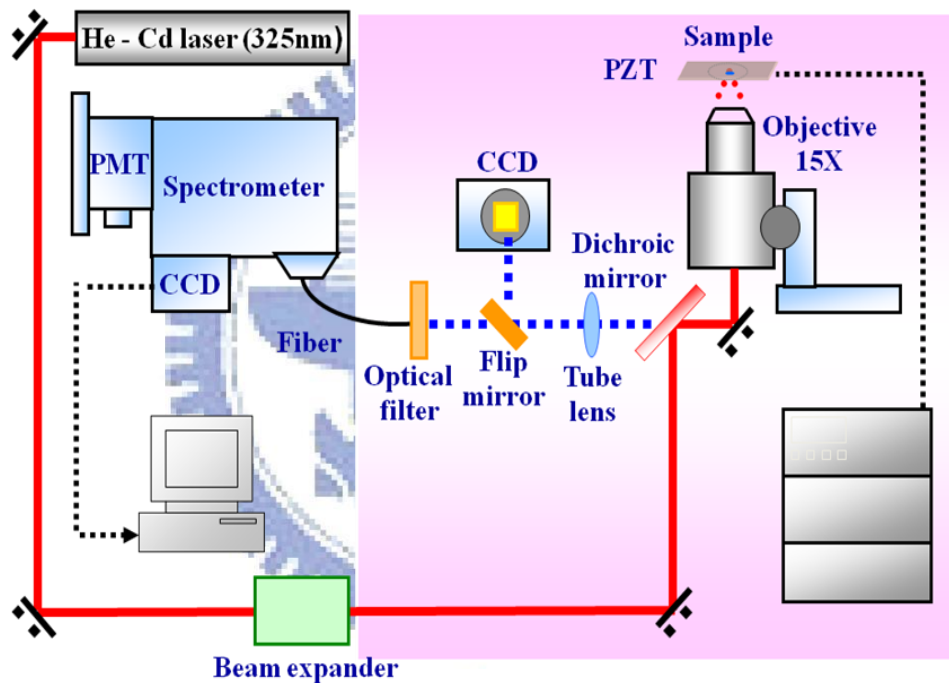


Fig. 3.1.1 The schematic of experimental Photoluminescence setup

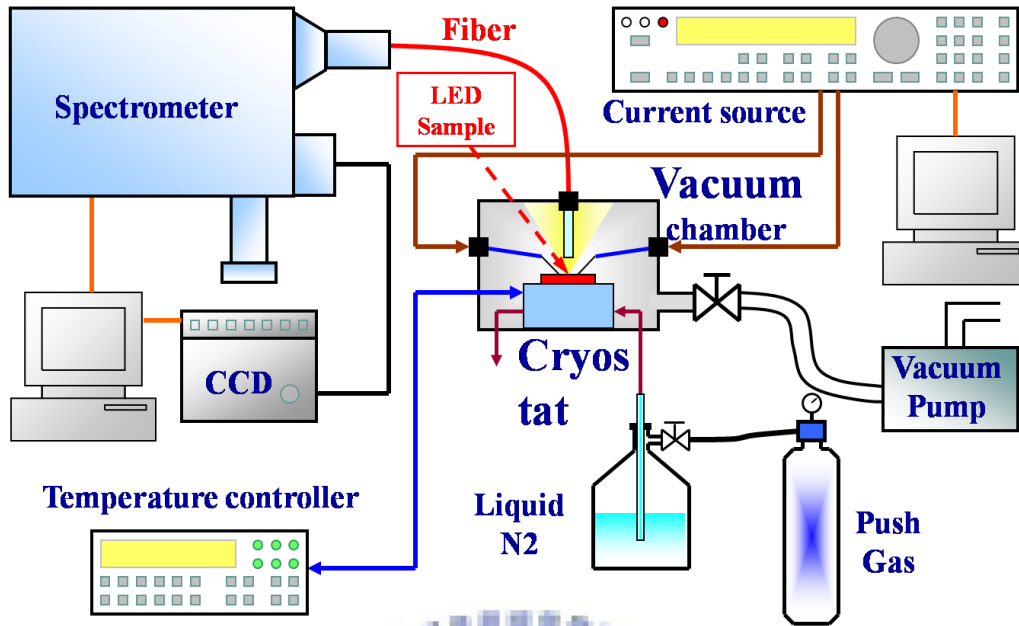


Fig. 3.2.1 The schematic of IQE measurement system

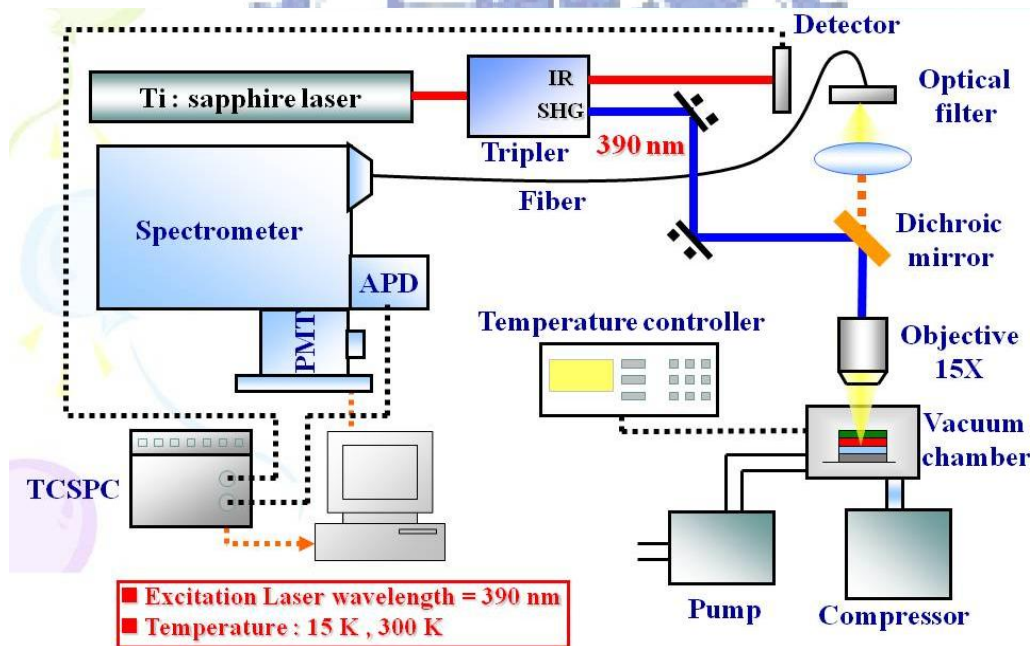


Fig. 3.3.1 The schematic of EL measurement system

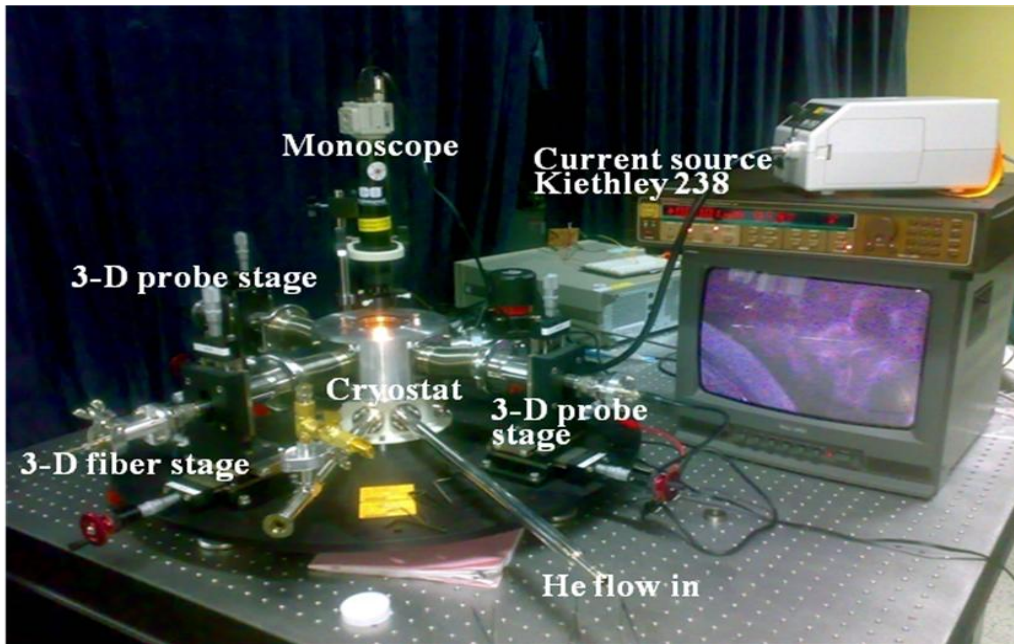
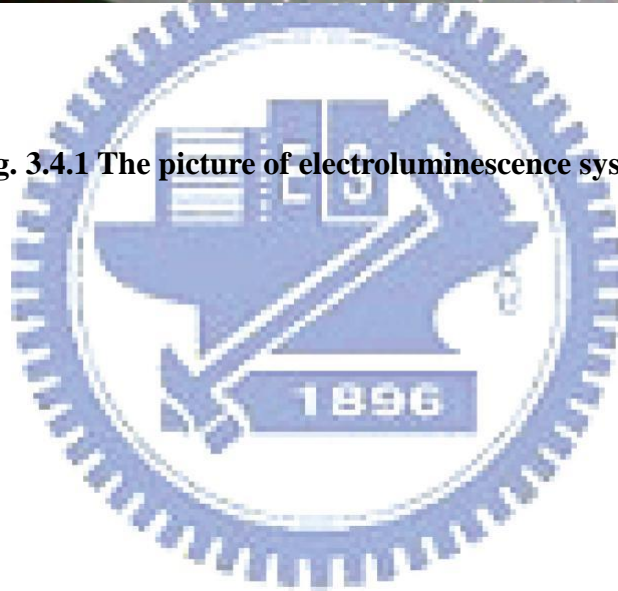


Fig. 3.4.1 The picture of electroluminescence system



Chapter 4 Optical and electrical properties of InGaN/GaN multiple quantum wells with and without prestrain layer

4-1 Introduction

Generally speaking, lattice constants in the lateral plane of the substrate and quantum well are different and there exist strains in one or both of components. The strains change the energy gaps, the curvature of the valence bands, and consequently, the effective masses of the holes. Therefore, the quantum confined valence subbands are modified by the biaxial strains. The biaxial strains also lead to the piezoelectric field along the Z direction in wurtzite materials. It inclines the one-dimensional confinement potential. The quantum confinement energy levels and the corresponding envelop function in such potential are different from those in the original confinement potential. This is easily understood that imaging the field pushes the electrons and the holes toward the opposite walls in the well because of opposite charges. Thus the overlap of the electron and hole wave function is reduced and this reduction is expected to result in the decrease of the exciton binding energy. Therefore, optical properties under the presence of the piezoelectric field are expected to be considerably modified from those in the absence it.

4-2 Sample structure and Fabrication

The sample in this study are commercial InGaN/GaN MQW LEDs and grown by metalorganic chemical vapor deposition (MOCVD). The sample in this study grown on *c*-plane (0001) sapphire substrates. The sample structure consist 2 μ m undoped n-GaN, a 2 μ m Si-doped *n*-type GaN, and an unintentionally doped active layer with In_xGa_{1-x}N/GaN MQWs, and a 20nm *p*-AlGa_{0.3}N electron blocking layer (EBL), and 120nm Mg-doped *p*-type GaN(Cladding layer). The doped concentration of *n*- and *p*-type GaN is nominally 5×10^{18} and 1×10^{19} cm⁻³, respectively, the MQWs layer comprise 6 periods InGa_{0.15}N well (~2.5 nm) and GaN barrier (~12 nm),in composition is 15%. In this study, LED samples with the InGa_{0.15}N/GaN insertion layer were labeled as LED-I, which comprise 10 periods InGa_{0.15}N layer(~1nm) and GaN layer(~5nm),in composition is 6%. Sample with a low temperature growth GaN prestrain layer was labeled as LED- II. The LT-GaN prestrain layer grown at 840 ° C, this growth condition has higher vertical-to-lateral growth rate ratio compared to a high growth temperature. This may allow LT-GaN layer to release strain from lattice mismatch. While LEDs without the insertion layer were also prepared for comparison and labeled as LED-III. The sample structure is shown in Fig. 4.2.1. The fabrication processes of InGaN/GaN LED show in Fig. 4.2.2 . In this study, we insert a prestrain layer between *n*-type GaN and MQW, which may release the strain cause

by the lattice mismatch between sapphire and GaN, In this study, an LT-GaN prestrain layer was used and compared with general InGaN/GaN prestrain layer. The difference between sample I and sample II may affect the internal quantum efficiency and the efficiency droop at high carrier density, hence, we will study the relation between localized state in quantum well and physical mechanisms of quantum efficiency.

4-3 CL image measurement and discussion

For this study, the spatially resolved CL images were obtained by scanning the scanning emission microscopy over the samples. The observed submicron-scaled CL inhomogeneities should be due to the spatial fluctuation of the energy band gap, which is mainly created by the spatial distribution of indium composition in InGaN active layers. Fig.4.3-1(a),(b),and(c) shows the top view CL images of LED with LED-I, LED-II, and LED-III. It can be seen clearly that emission pattern of (b) and (c) were both inhomogeneous. In contrast, Sample with LT-GaN prestrain layers has the most uniform emission image at corresponding peak emission wavelength. The various emission area observed from sample with prestrain layers and without prestrain layers indicate that elastic relaxation occurred in the prestrain layers by surface undulations. Since the indium segregation to form emission pattern inhomogeneous is energetically favored by reducing the number of compressively

strained In–N bonds, indium atoms can preferentially segregate to the ridges from the troughs of the undulated surface. As a result, In-rich regions will be formed near the surface. Therefore, the density of In-rich regions in InGaN/GaN prestrain layers was larger than that in LT-GaN prestrain layers. This will result in the formation of In-rich regions due to these In-rich surface.

4-4 Power dependent PL measurement

4-4.1 Carrier localization effect

Due to composition inhomogeneity and monolayer thickness fluctuation Of InGaN QWs self-organized In-rich region is generated in InGaN active region, resulting in potential fluctuation of energy bandgap. AS shown in Fig.4.4.1.1 As injected carrier density increases further, an occupation of high energy states of localized centers will be enhanced. And the band filling effect will make the carriers more easily escape from localized states to extended states which decrease IQE.

From the Fig 4.4.1.2 we could found that LED without prestrain layer structure has much higher FWHM under the same carrier density. At carrier density above 1×10^{18} (#/cm³), the FWHM increase fast and the band filling effect is start to dominate. From Fig 4.4.2, we can see sample III has larger FWHM than others, which means In distribution is the most inhomogeneous and more nonradiative center in quantum well.

On the other hand, the LT-GaN and InGaN/GaN prestrain sample has similar band width at low carrier density. However, as carrier density above 1×10^{18} ($\#/cm^3$), the sample with LT-GaN prestrain layer has smaller band width than InGaN/GaN prestrain layer which means smaller band filling effect. The possible reason of reducing In fluctuation of LT-GaN prestrain layer sample may relating to using GaN film can more effectively eliminate In incorporation in active regions than InGaN film.

4-4.2 Reduction of pizeoelectric field

Several research groups have reported that the internal electric field existed in InGaN/GaN QW structure. This internal electric field through the QW tilts the potential band and leads to a spatial separation of electrons and holes in the QW, resulting a decreasing in degreed of wave function overlap which is called the QCSE.

The internal electric filed in the QW can be screened by photogenerated carriers. Consequently, the QCSE effect become weaker when the carrier density increased, resulting in the emission peak wavelength buleshift and IQE enhanced at low injected carriers region. . Figure 4.4.2.1 shows the emission peak energy under different input power. When the input power was increase, the peak energy of the emission spectra of the LEDs changed to larger energy. The blue shift of three sample with increasing

input power before 10mW may be explained by the carrier screening of the QCSE resulting from piezoelectric fields.[45][46] When the prestrain layer was inserted between n-GaN and MQW, the blue shift by screen effect are decrease from 20meV to only 10meV. We now analyze the spontaneous PL in the InGaN samples in more detail. We explain the PL behavior differences of the LED with and without prestrain layer by quantum confinement and the predominant strong piezoelectric field in thin quantum wells. Indeed, in hexagonal nitride MQWs, the quantum-confined Stark effect arises due to the piezoelectric field.[46] We analyzed the influence of nonequilibrium carriers on the position of PL spectra in the InGaN/GaN MQWs using a triangular well model. The photoexcited carriers screen the internal field. For an idealized case, neglecting thermal distribution in the bands, the emitted quantum energy $h\nu$ for band-to-band recombination in a quantum well in the presence of nonequilibrium electron-hole pair density n can be expressed as $h\nu = E_g(n) - edF(n) + E_e(n) + E_h(n)$. Here, $E_g(n)$ is the carrier density dependent forbidden gap, which, taking into account band-gap renormalization, can be expressed as $E_g(n) = E_g(0) - \beta n^{\frac{1}{3}}$ with $\beta = 2 \times 10^{-8}$ eV cm; d is the well width; $F(n)$ is the internal electric field strength, which can be expressed as $F(n) \approx F(0) - \frac{ned}{\epsilon\epsilon_0}$ with maximum field strength $F(0)$ and static relative dielectric constant ϵ , which has been taken as 10; and $E_{e,h}$ is the difference of the lowest-energy level from the

triangular well bottom for electrons and holes, respectively, and can be calculated

from $E_{e,h} \cong \left(\frac{\hbar^2}{2m_{e,h}}\right)^{1/3} \left[\frac{9\pi F(n)}{8}\right]^{2/3}$. The effective masses of electrons or holes, $m_{e,h}$,

used in the calculations have been assumed to be $0.25m_0$, $m_h > m_0$, respectively[47].

In order to compare our experimental results with the calculations, we expressed $h\nu$ as

a function of excitation power density P (in MW/cm²), which for the case of

predominantly square-law recombination are related as[48] $n = n = \sqrt{P\alpha/h\nu\gamma}$, where

α is the absorption coefficient for laser light and has been taken as 1.5×10^5 cm⁻², and γ

is the square-law recombination coefficient and has been taken as[49] 4.8×10^{-11} cm³

s⁻¹.

The results of these calculations for InGaN/GaN MQWs are also illustrated in Figure 4.4.2.1 by the dotted line. This rather crude model gives remarkably good

agreement between experimental data and theoretical estimations for more than four

orders of excitation power density (up to 10 kW/cm²). Note that a number of other

effects were not included in our model (we neglected the two-dimensional nature of

the system, carrier distribution in the barriers and the wells, excitonic and

nonradiative recombination channels, possible recombination coefficient change due

to separation of the carriers in wells, etc.). The F_0 of reference was found to be equal

to 1.21 V/cm, which is quite similar to other evaluations in similar semiconductor

structures.[48] The estimation of the piezoelectric field of sample I and sample II are

the value of 0.68 and 0.73MV/cm, which is much smaller than sample III. From the above experiment result and data analysis, we can conclude that the use of LT-GaN prestrain layer release the biaxial strain in quantum well for a certainty.

4-5 Temperature dependent PL measurement

In order to further clarify the influence of the carrier confinement ability of LED with and without prestrain layer, temperature dependent PL measurements were performed. The Fig. 4.5.1 shows Arrhenius plots of the normalized integrated PL intensity for the InGaN-related PL emission over the temperature range from 20K to 300K. It was found that the integrated PL intensity dropped slowly with temperature during the low-temperature region, whereas it decreased rapidly during the high-temperature region. The best fitting gives three activation energies of about 51, 45, and 32 meV for InGaN/GaN, LT-GAN, and without prestrain layer, respectively.

In general, the quenching of the luminescence with temperature can be explained by thermal emission of the carriers out of a confining potential with an activation energy correlated with the depth of the confining potential [49]. It has suggested that the localization of carriers operates as excellent radiative recombination centers. In other words, high localization energies of excitons will provide deep potential wells that suppress the diffusion of electrical carriers toward various non-radiative defects. The

carrier localization in the active layer also has a significant effect on the performance of LEDs, resulting in an increase in radiative recombination efficiencies[50].

4-6 The measurement of internal quantum efficiency

From the preview result, we know that LT-GaN prestrain did change the property of active region. For this study, we used the IQE method which S. Watanabe *et al.* proposed to determine the IQE of InGaN/GaN MQW LEDs to study the IQE of different structure. The internal quantum efficiency can be calculated by

$$\eta_{PL} = C \frac{I_{PL} / E_{PL}}{I_{EX} / E_{EX}} \quad (4.6.1)$$

where I_{PL} and I_{EX} are PL intensity and excitation intensity, respectively. E_{PL} and E_{EX} are PL photon energy and excitation photon energy, respectively. C is a constant affected by mostly carrier injection efficiency by laser, light extraction and correction efficiency of PL, and does not depend on either excitation power density or measurement temperature. First, we measured the excitation power dependent PL intensity at low and room temperature, and then the relative PL quantum efficiency curves can be obtained by using equation 4.6.1. And the constant C would be canceled out by normalizing the curves to the peak value at the lowest temperature, because it is independent on temperature or excitation power. From this normalization, the PL

efficiency curves will not depend on carrier injection efficiency by laser, light extraction and correction efficiency of PL. Therefore, the PL efficiency would be find out from this model.

In tradition, the IQE is estimated by assuming that IQE is 100 % at low temperature regardless of excitation power density. However, IQE is strongly dependent on injected carrier density. Consequently, it is more reasonable to assume the peak of PL efficiency at lowest temperature is equal 100 %, and then the IQE curves as a function of excitation power and temperature can be understand.

Moreover, to avoid the absorption of GaN, the frequency doubled femtosecond pulse Ti: sapphire laser of 390 nm was used to excite sample, the excitation power density was changed from 0.01 to 80 mW, and calculated injection carrier density is about 2.0×10^{15} to $1.6 \times 10^{18} \text{ cm}^{-3}$ by using the equation below:

$$\text{carrier density} = \frac{P}{(h\nu) * \phi * d_{\text{active}} * f} * \exp(-\alpha_{\text{GaN}} d_{\text{GaN}}) * (1 - \exp(-\alpha_{\text{InGaN}} d_{\text{active}})) R * \text{loss}_{\text{objective}} \quad (4.6.2)$$

where P is excitation power, $h\nu$ is energy of incident light, ϕ is laser spot size, f is repetition rate of laser, d_{active} is the active layer thickness, α_{GaN} is the absorption of GaN, α_{InGaN} is absorption of InGaN, R is reflection of sample surface, and $\text{Loss}_{\text{objective}}$ is transmission loss of objective.

Fig. 4.6.1 shows the IQE of InGaN/GaN MQW LEDs as a function of injected

carrier density at 15K and 300 K. We can observe that the IQE increases with increasing injected carrier density to reach its maximum. As injected carrier density further increases, then the IQE decreases. The tendency of two efficiency curves at 15 K and 300 K is very similar. But under low injected carrier density region, the IQE curve at 300 K increases obviously than it at 15 K. The results indicated that the IQE at 15 K saturated more easily than it at 300 K.

The experimental results indicated that the IQE are about 61.9 %, 41.4 % and 53.6% at injected carrier density is $4.7 \times 10^{17} \text{ #/cm}^3$ (~20mA) for sample I, sample II and sample III, respectively. Table 4.6.1 shows the value of IQE, We believe the higher internal quantum efficiency for the LED is due to the better crystalline quality, attributed to reducing of threading dislocations and releasing strain from sapphire ,so enhance the carrier confinement ability as studied in previous work [51]. However, when carrier density increase to $1.6 \times 10^{18} \text{ #/cm}^3$,the IQE are about 33.9 %,and 51.1 % for LED with InGaN/GaN and LT-GaN prestrain layer. Under similar quality and strain release order, the LED with LT-GaN insertion layer has much higher efficiency than InGaN/GaN is due to better In distribution and less nonradiative center.

4-7 Current dependent intensity and efficiency discussion

Fig.4.7.1 shows the light output power versus injection current ($L-I$) characteristics of these LED samples. When a 20-mA current injection was applied to the LEDs with emitting wavelength of 460 nm, the output powers enhancement of LED-I and LED-II were approximately 11% and 18%, respectively. Even InGaN/GaN LED has higher output power enhancement at 20mA, as injection current increase to 200mA, the LT-GaN LED has larger output power enhancement than InGaN/GaN LEDs. In addition to the improvement of light output power for the LED. Note that three samples, regardless of having InGaN/GaN, LT-GaN or without prestrain layer between active region and n-type GaN show almost the same current density dependency of forward voltage. As shown in Fig. 4.7.2, the EQE rapidly decreases as the forward current increases up to 200mA, resulting in the serious EQE droop of ~54%. However, the MQW LEDs with LT-GaN prestrain layer show very different dependency of the EQE on the forward current density, EQE very slowly decreases with increasing the forward current density, showing the magnitude of EQE droop of approximately 36% at J_f of 200 mA. Table 4.7.1 shows the value of output power enhancement and efficiency decrease. These results indicate that LT-GaN prestrain layer facilitate the suppression of In inhomogeneous distribution in the active region , and successfully enhance the power and efficiency at high carrier density.

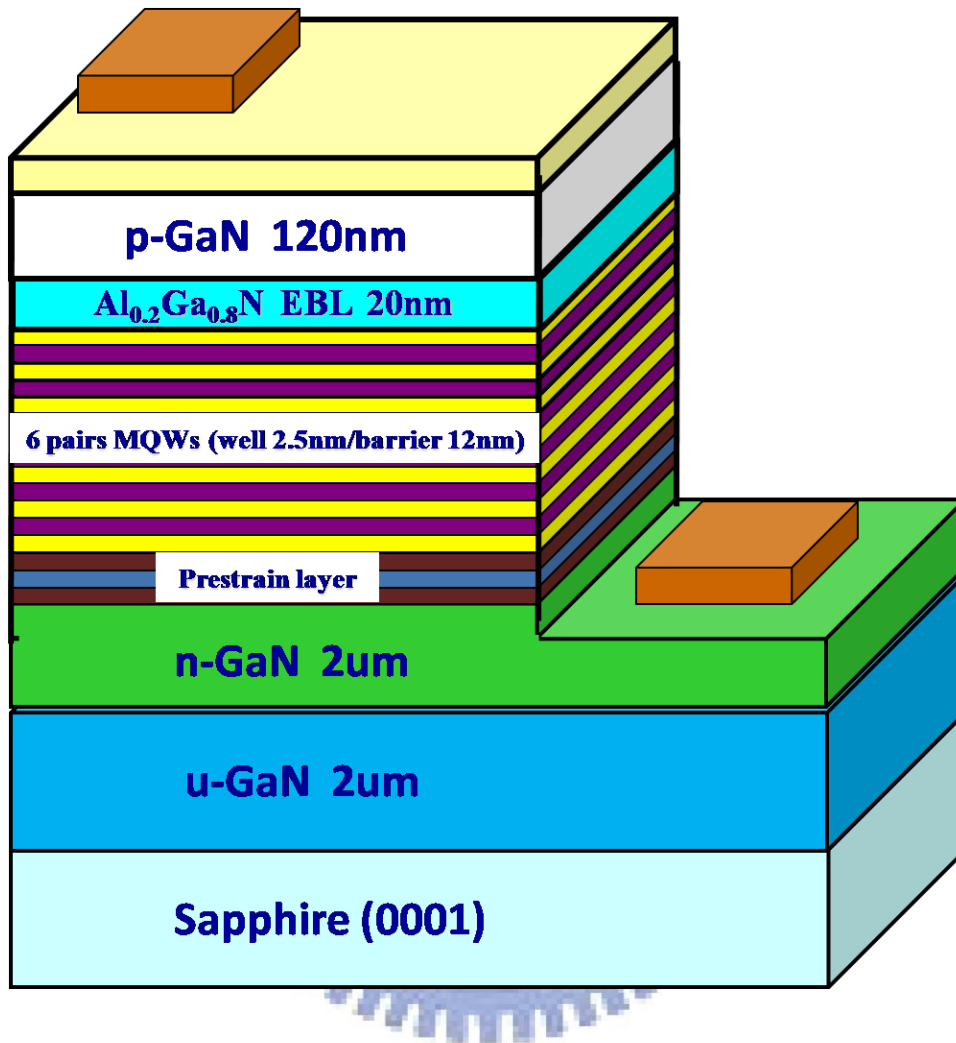


Figure.. 4.2.1 The schematic drawing of sample structure

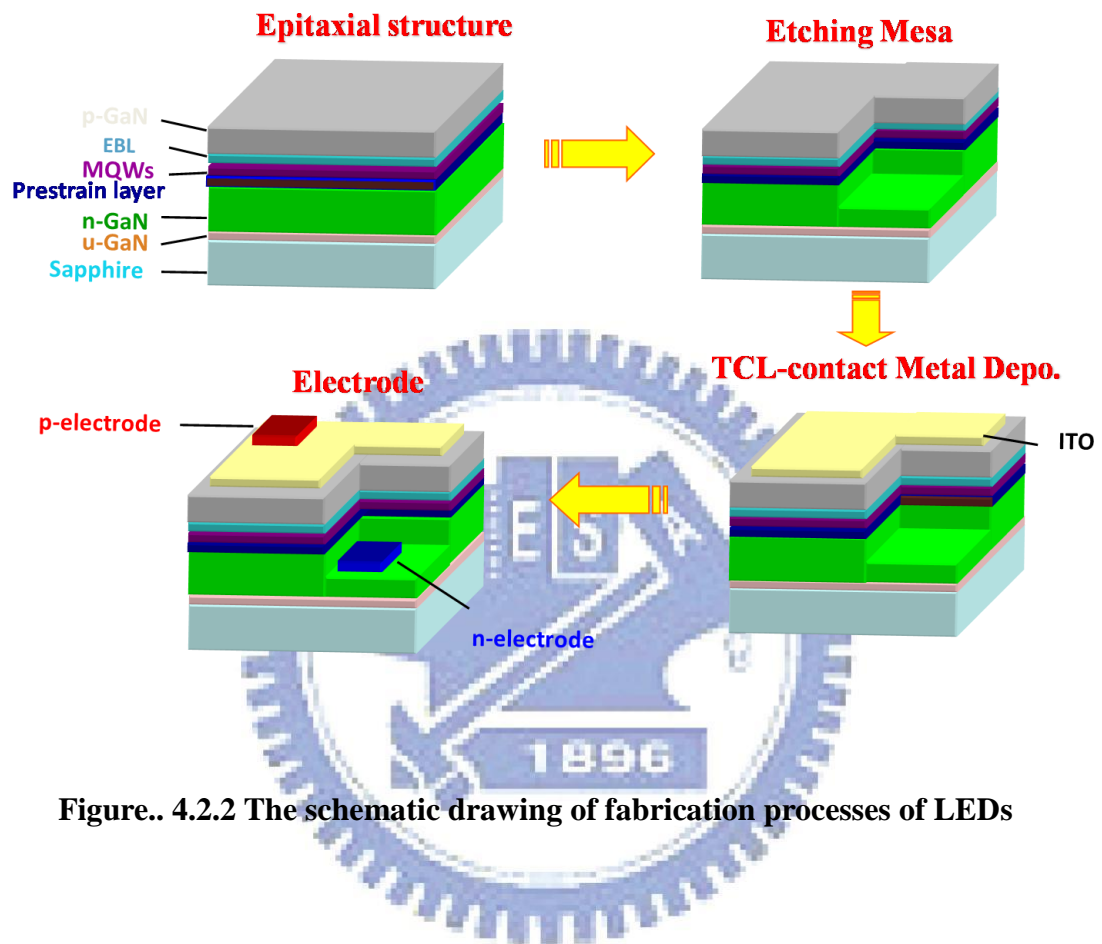


Figure.. 4.2.2 The schematic drawing of fabrication processes of LEDs

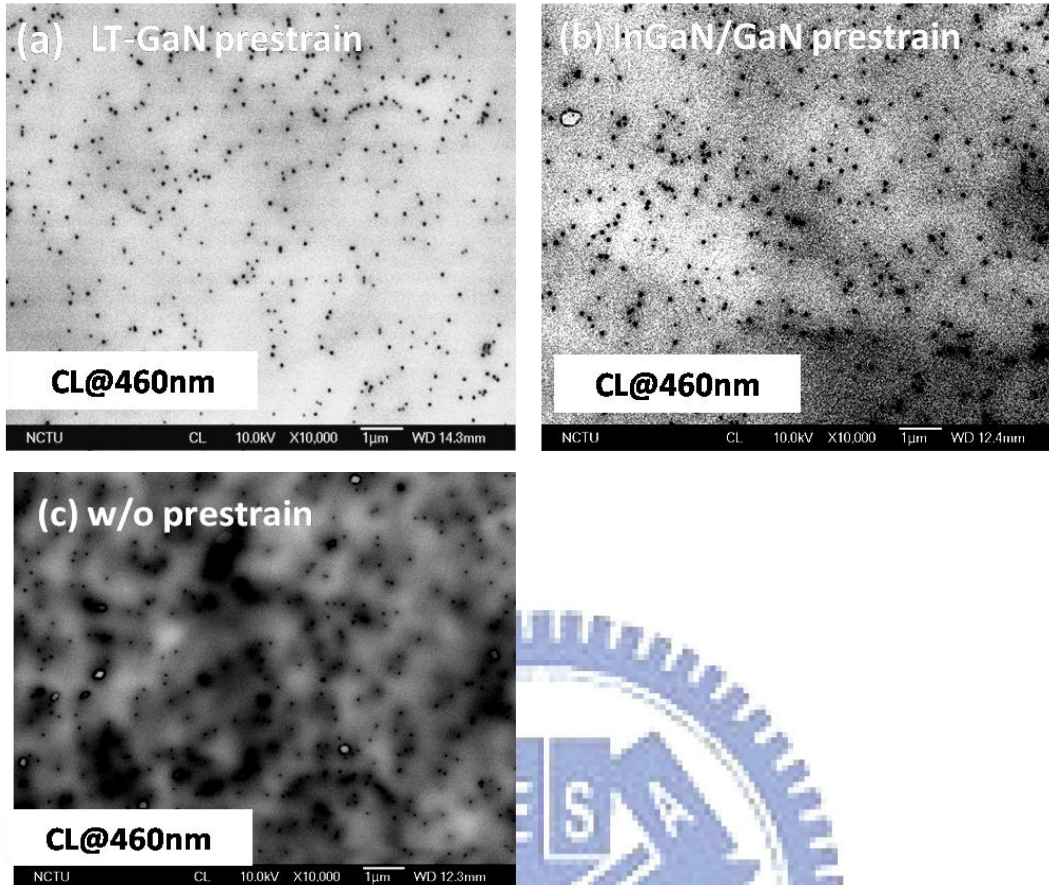


Figure. 4.3.1 Top view CL images of (a) LT-GaN prestrain layer, (b) InGaN/GaN prestrain (c) w/o prestrain structure at corresponding emission peak wavelength

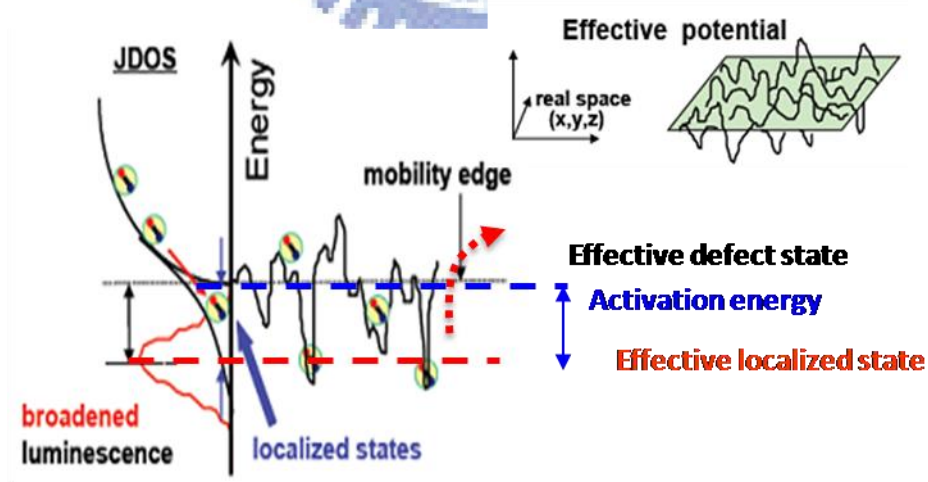


Figure. 4.4.1.1 Schematic band diagrams of localized state due to In fluctuation

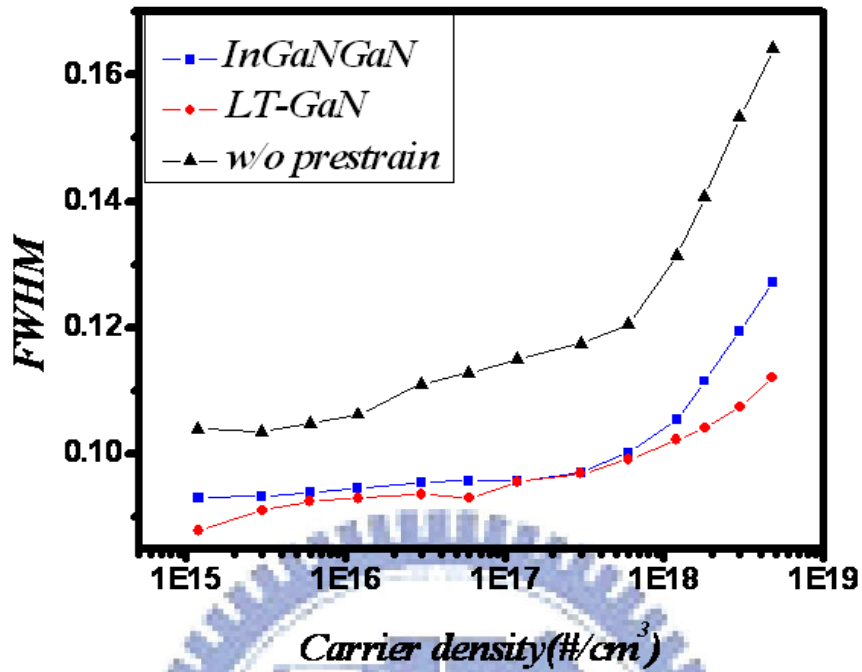


Figure. 4.4.1.2 FWHM of three samples at different carrier density

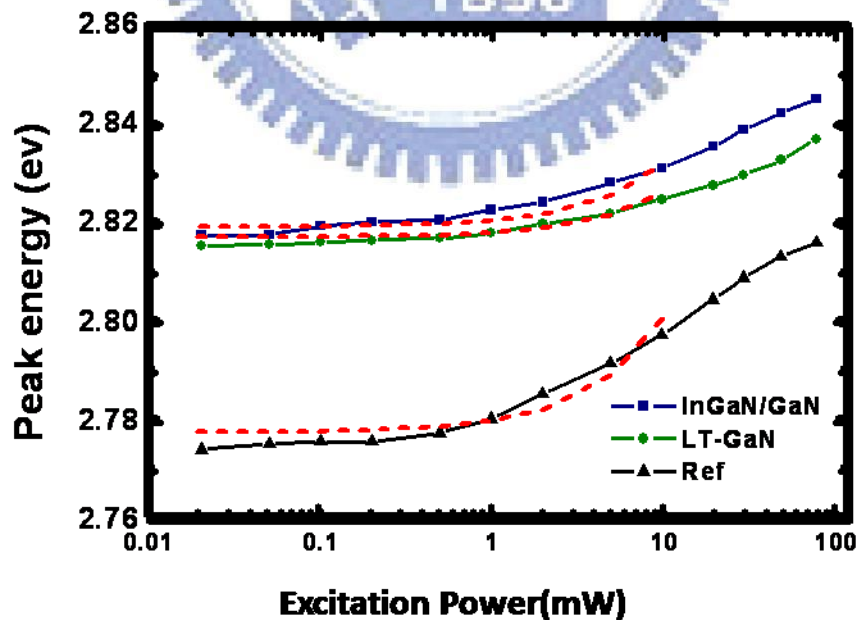


Figure. 4.4.2.1 Emission energy of (a)LT-GaN (b)InGaN/GaN (c)w/o prestrain structure at different power density.

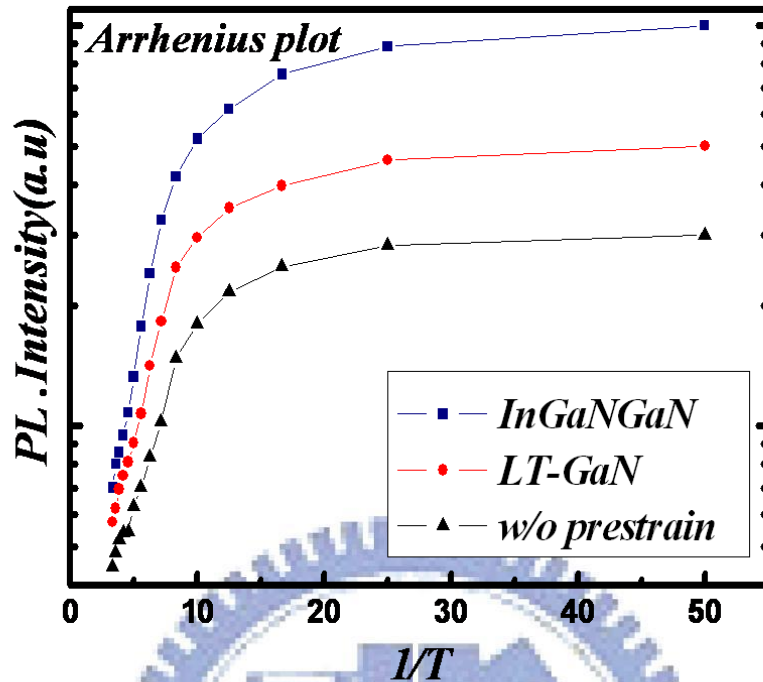


Figure. 4.5.1 The Arrhenius plot of the integrated PL intensity obtained from the main emission peak over the temperature range from 10 to 300 K.

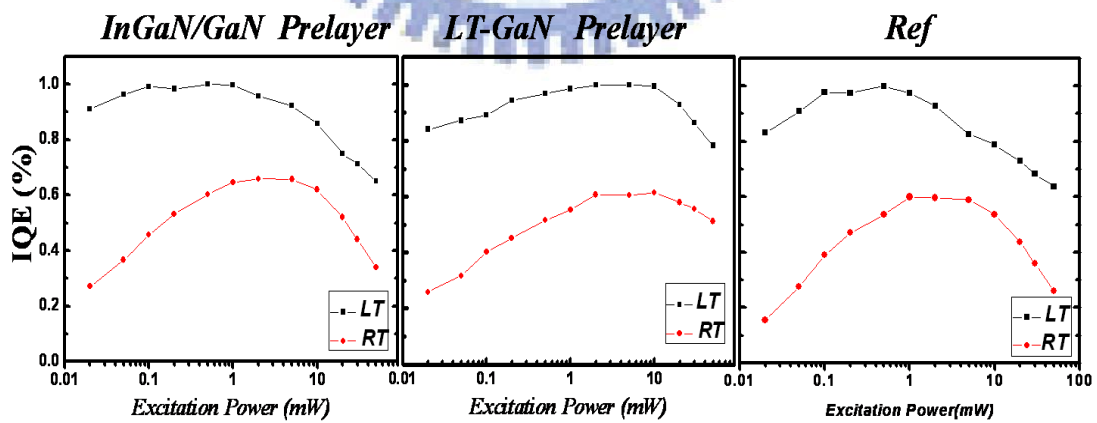


Figure. 4.6.1 IQE as a function of excitation power at 15K and 300 K.

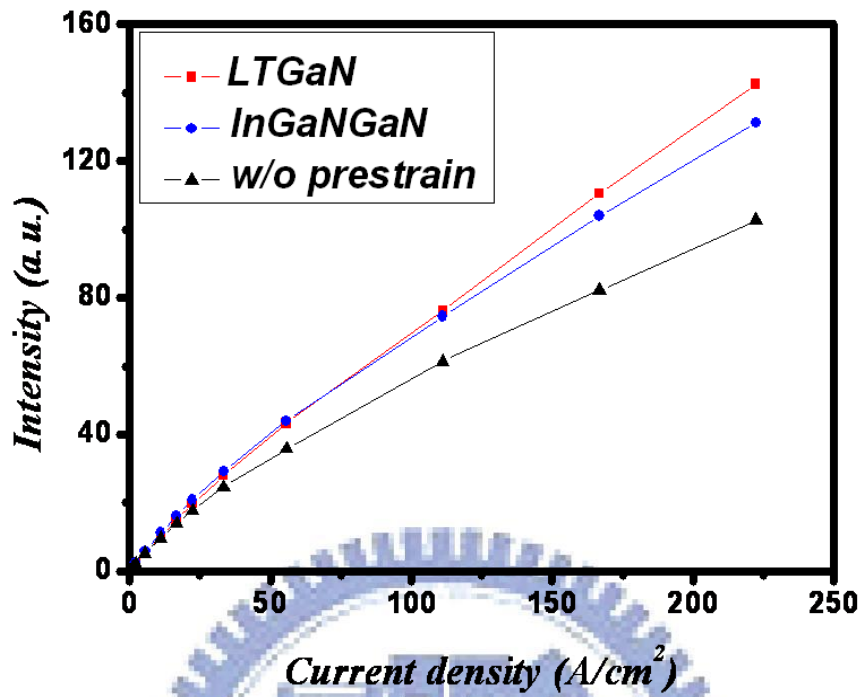


Figure. 4.7.1 Emission power as a function of current density of three sample

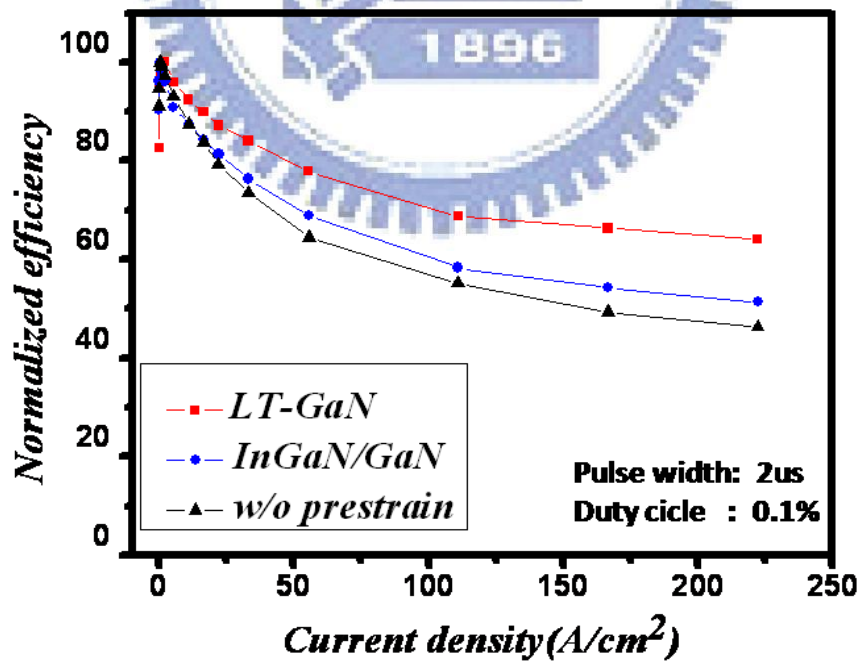


Figure. 4.7.2 Emission efficiency as a function of current density

Table 4.6.1 IQE of InGaN/GaN, LT-GaN and without prestrain layers**InGaN/GaN LED at 10 and 80mW**

Sample	PL IQE @10mW(%)	PL IQE @80mW(%)
LT-GaN	~ 61.4%	~51.1%
InGaN/GaN	~ 61.9 %	~33.9%
w/o prestrain	~53.6%	~26.0%

Table 4.7.1 Output power enhance and efficiency decrease

Sample	Output power enhance (%)		Efficiency droop(%)
	20mA	200mA	Max~200mA
LT-GaN	~11%	~39%	36%
InGaN/GaN	~18%	~28%	49%

Chapter 5 Analysis of the reduce efficiency droop by Graded quantum wells structure

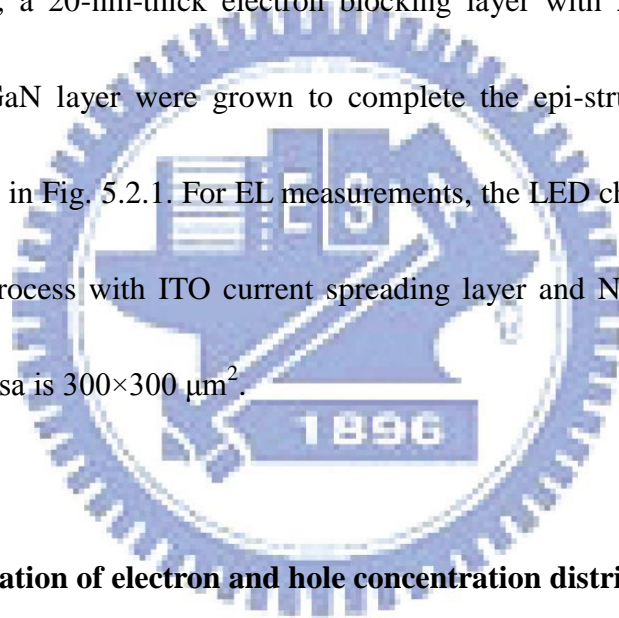
5-1 Introduction

In recent years, great efforts have been made to reduce the efficiency droop. Most of them are focus on minimizing the carrier overflow by reduce or eliminate the polarization field in the active region, such as using polarization matched multiple quantum wells (MQWs) [52, 53], staggered InGaN quantum wells [54], and non-polar or semi-polar GaN substrate [55]. But for improving hole distribution, only several approaches, such as *p*-type MQWs [56] or coupled quantum wells [57], are explored. However, in the *p*-type MQWs, the Mg-dopant is very likely to diffuse into wells, while in the coupled quantum wells, electrons are tend to overflow by using thin barriers. These will result in reduction of radiative efficiency. In this research, we designed and grew a new LED structure with graded-thickness multiple quantum wells (GQWs) by using metal-organic chemical vapor deposition (MOCVD). Better hole distribution in such graded-thickness designed MQWs were demonstrated by APSYS simulation as well as the electroluminescence (EL) measurements.

5-2 Sample structure and fabrication

The LED structures were grown on c-plane sapphire substrates by MOCVD. A 20-nm-thick low temperature GaN nucleation layer followed by a 2 μm *n*-type GaN

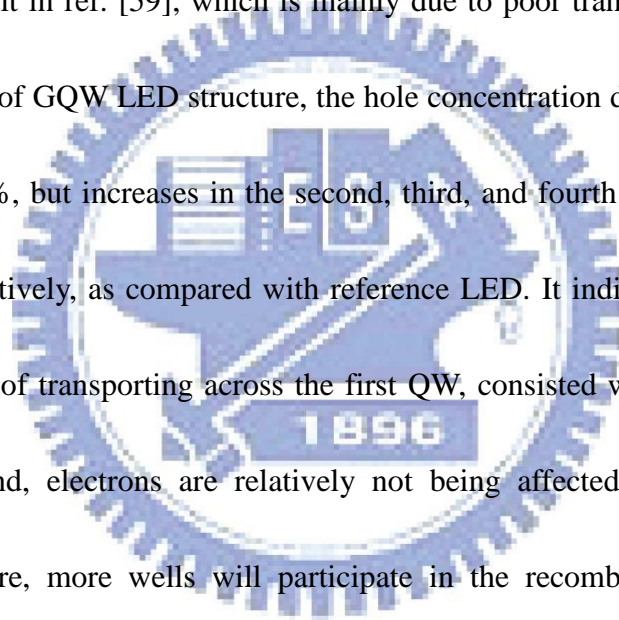
buffer layer, ten-pair InGaN/GaN superlattice were grown on the top of sapphire. After that, six-pair MQWs were grown with 10-nm-thick GaN barriers. For our designed experiment, the thicknesses of In_{0.15}Ga_{0.85}N quantum wells for GQW LED structure, controlled by growth time, are 1.5, 1.8, 2.1, 2.4, 2.7, 3 nm along [0001] direction. While the reference LED structure has a unique well-thickness of 2.25 nm. It's worth noting here that the total volumes of active region for the two samples are the same. Finally, a 20-nm-thick electron blocking layer with Al_{0.15}Ga_{0.85}N and a 120-nm-thick *p*-GaN layer were grown to complete the epi-structure. The sample structure is shown in Fig. 5.2.1. For EL measurements, the LED chips were fabricated by regular chip process with ITO current spreading layer and Ni/Au contact metal, and the size of mesa is 300×300 μm².



5-3 APSYS simulation of electron and hole concentration distribution

Based on our experimental structures, we built up the model of the reference and GQW LED structures. The typical LED structure was composed of 2-μm-thick *n*-type GaN layer (n -doping=2E18 cm⁻³), six pairs of In_{0.15}Ga_{0.85}N/GaN MQWs with 10-nm-thick GaN barriers, 20-nm-thick *p*-Al_{0.15}Ga_{0.85}N electron blocking layer (p -doping=5E17 cm⁻³), and 120-nm-thick *p*-type GaN layer (p -doping=1E18 cm⁻³). Other material parameters of the semiconductors used in the simulation can be found

in Ref. [58]. Commonly accepted Shockley-Read-Hall recombination lifetime parameters (several nano-seconds) are used in the simulations. Figure 5.3.1 and Figure 5.3.2 shows the simulated hole distribution and radiative recombination distribution along MQWs at 100 A/cm^2 . For reference LED structure, it can clearly be seen that holes mostly concentrate in the QW nearest p -side (denoted as the first QW), so does the radiative recombination. This phenomenon coincides with the optical measurement result in ref. [59], which is mainly due to poor transportation of holes. While in the case of GQW LED structure, the hole concentration decreases in the first QW by about 16%, but increases in the second, third, and fourth QWs by 7%, 94%, and 175%, respectively, as compared with reference LED. It indicates that the holes are more capable of transporting across the first QW, consisted with our hypothesis. On the other hand, electrons are relatively not being affected due to their high mobility. Therefore, more wells will participate in the recombination process, as illustrated by the radiative recombination distribution in Fig.5.3.2 Moreover, due to the relative low carrier densities in the first QW and more uniform of carrier distribution, the possibility of Auger scattering and carrier overflow can be lower. Accordingly, alleviation of efficiency droop can be expected.



5-4 Current dependent electroluminescence measurement and analysis

The electroluminescence EL spectra of the LEDs were measured using a pulsed current source with 1% duty cycle and 2 μ s pulse width, to eliminate the heating effect. Light was collected by an optical fiber placed above the diode and connected to a computer controlled spectrometer equipped with a charge coupled device detector.

Different well width has different emission energy, so the GQW LED has larger band width than reference LED at whole current range. And which has been mentioned before is LED with thicker QW will emission longer wavelength due to QCSE effect. So, The emission energy of GQW LED is smaller than reference LED at small current density, as the injection increase, the peak energy will increase with injection current due to band filling effect, and the GQW LED has larger emission energy at high current density. Under the same current density, LED with thicker well width should have smaller peak energy (small band filling effect), however, in our experiment, the GQW LED has inverted result, which means carrier might transfer from the widest well width QW to thinner well width QW close to n-type GaN. Therefore we can conclude that graded quantum does have better carrier transport ability.

According to the simulated results mentioned above, more holes distribute in the narrower wells in GQW LED structure. Once more carriers radiatively recombine in

narrower well, the intensity of shorter-wavelength part in emission spectrum will rise. Thus, the symmetry of spectrum might be changed, as can be seen from the power dependent of EL spectrum in Fig. 5.4.1. To investigate EL spectrum in detail, the asymmetry factor (AsF) was calculated. As illustrated inset of Fig.5.4.3, it can be defined as the distance from the center line of the peak to the back slope (AB) divided by twice the distance from the center line of the peak to the front slope (2AC), with all measurements made at 50% of the maximum peak height. The calculated AsF under every injection level for both samples are summarized in Fig. 5.4.2. It can clearly be seen that, AsF of reference LED decreases slightly from 1.04 to be about 0.98 when injection current increases from 1 A/cm² to 100 A/cm². While GQW LED shows larger variation, the AsF starts at 1.05 (0.1 A/cm²) and saturates at about 0.89 (after 20 A/cm²). According to the definition of AsF, if the bluer light emits from narrower wells, the symmetry of spectrum would be interrupted and smaller than 1.

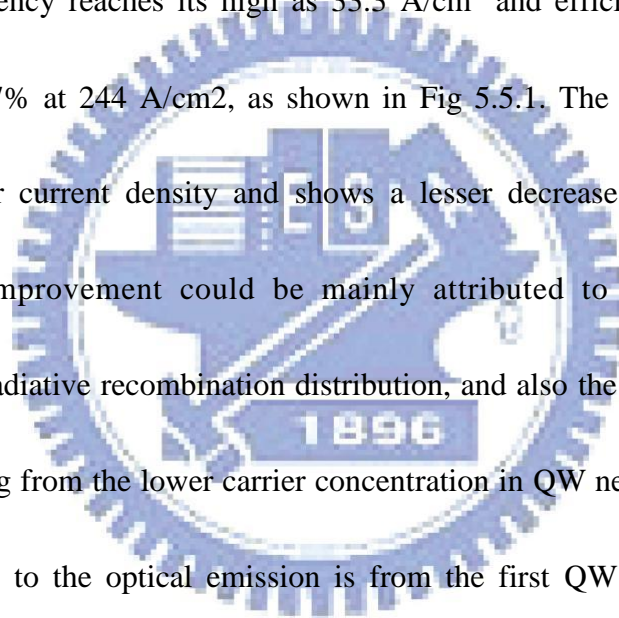
To further study the mechanisms responsible for the variation of the graded quantum structure, more electrical properties were investigated as below. Fig.5.4.3 shows the emission peak energy (a) and FWHM (b) of spectra as a function of the injected carrier density at room temperature for both LEDs of graded quantum well and reference. In Fig.5.4.3 several unique optical properties were observed. First, the emission peak energy gradually increases with the injected carrier density, this is due

to screening effect and band filling effect. And we can see, at low injection current, GQW LED has smaller emission peak energy and larger FWHM. The reason is when LED is under low injection current, only the quantum well which closest to p-type GaN generate light, and the GQW one has wider well width than reference. However, at high current density, we can observe the emission energy of GQW is larger than reference, it is due to carrier transport to thinner well which close to n-type GaN and emission short wavelength of GQW LED. The rapidly increase in FWHM of GQW also prove this penominace. Therefore, we can conclude that GQW does have superior radiative recombination distribution, which leads to the EL spectrum blueshifts and broadens significantly with increasing the injection current.

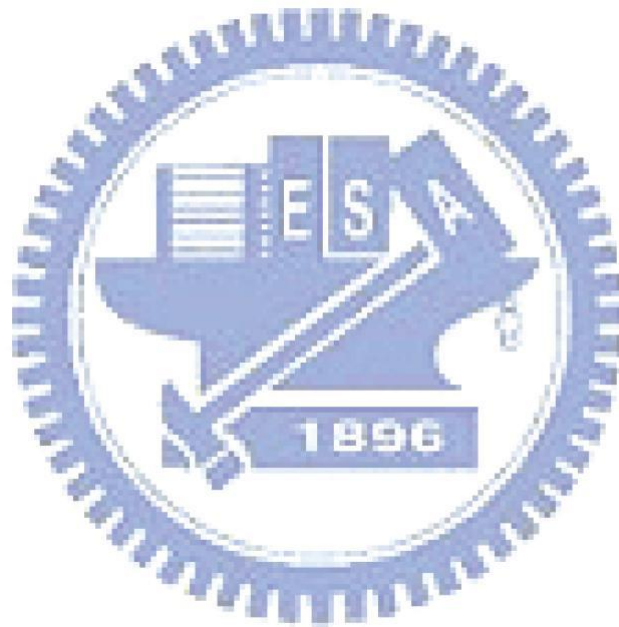
5-5 Analysis of injection carrier density dependence EL efficiency and efficiency droop

Finally, we investigated the efficiency droop behaviors in both LEDs. The output powers of LEDs and the normalized efficiency (η) of refrence and GQW LED are plotted in Fig. 5.5.1 as a function of injection current, which are obtained by integrating the light intensity of EL spectrum measured by spectrometer. The electroluminescence EL spectra of the LEDs were easured using a pulsed current source with 1% duty cycle and 2us pulse width, to eliminate the heating effect. Light was collected by an optical fiber placed above the diode and connected to a

computer controlled spectrometer equipped with a charge coupled device detector. It can clearly be seen that the light output power enhancement at current density of 22 A/cm² and 244 A/cm² for GQW LED is 36% and 71%. This indicates that even with wider wells (worse wave function overlap for electrons and holes) near p-side, the overall efficiency for GQW LED is still higher than reference, and the utilization rate of MQWs is improved. More importantly, LED without any structure, the relative efficiency reaches its high as 33.3 A/cm² and efficiency shows only a slight decrease 17% at 244 A/cm², as shown in Fig 5.5.1. The quantum efficiency peaks at a higher current density and shows a lesser decrease as current density increase. This improvement could be mainly attributed to the superior hole distribution and radiative recombination distribution, and also the reduction of Auger scattering resulting from the lower carrier concentration in QW nearest p-side. As the main contribution to the optical emission is from the first QW next to the p-type region. In fact, Li *et al* reported a shift of EQE peak position from 5 A/cm² to over 200 A/cm², but with a trade-off for the IQE, by widening QWs from 0.6 to 1.5 nm. This observation, not the interpretation, is actually consistent with the report by Gardner *et al.* in which case EQE reached its peak above 200 A/cm² when the MQW active layer was replaced by a double heterostructure with a 13 nm InGaN layer. This was, however, interpreted by authors as avoiding/minimizing Auger recombination by



reducing the carrier density in the wells. Furthermore, for the samples with graded quantum well. It should be noted that despite the pulsed measurements and pushing of the efficiency peak to higher currents, the droop is still affected by heating since a red shift not shown of the EL peak position beyond 300 A/cm² is observed.



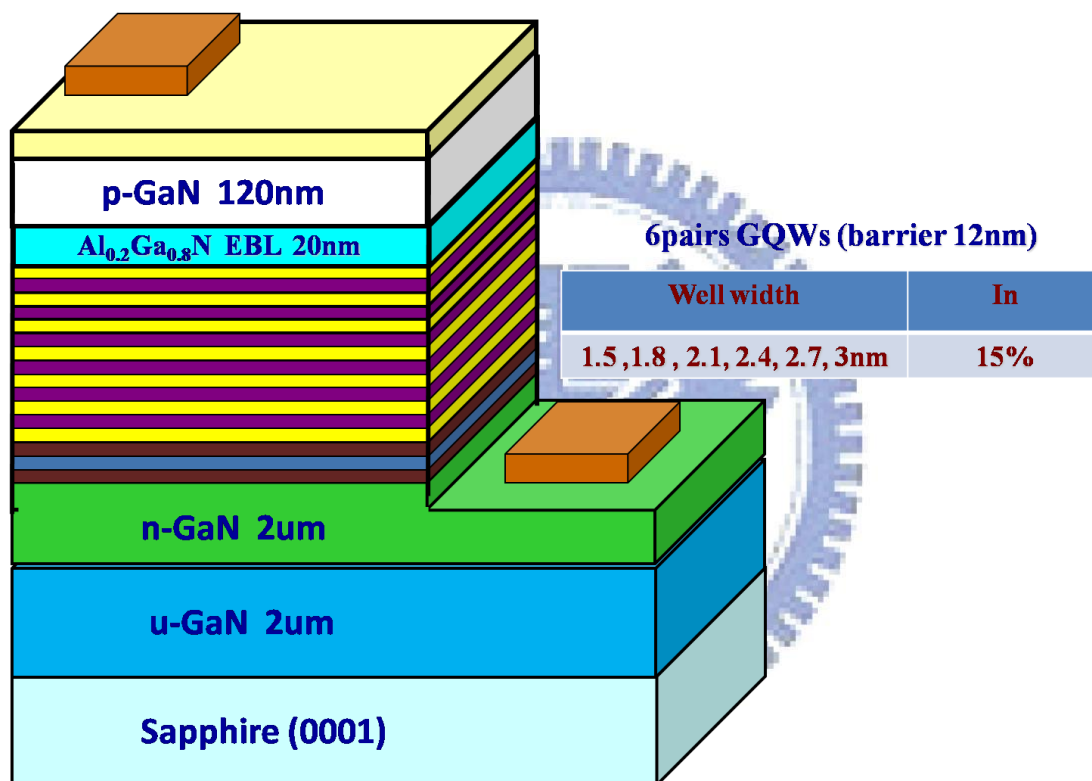


Figure. 5.2.1 The schematic drawing of sample structure

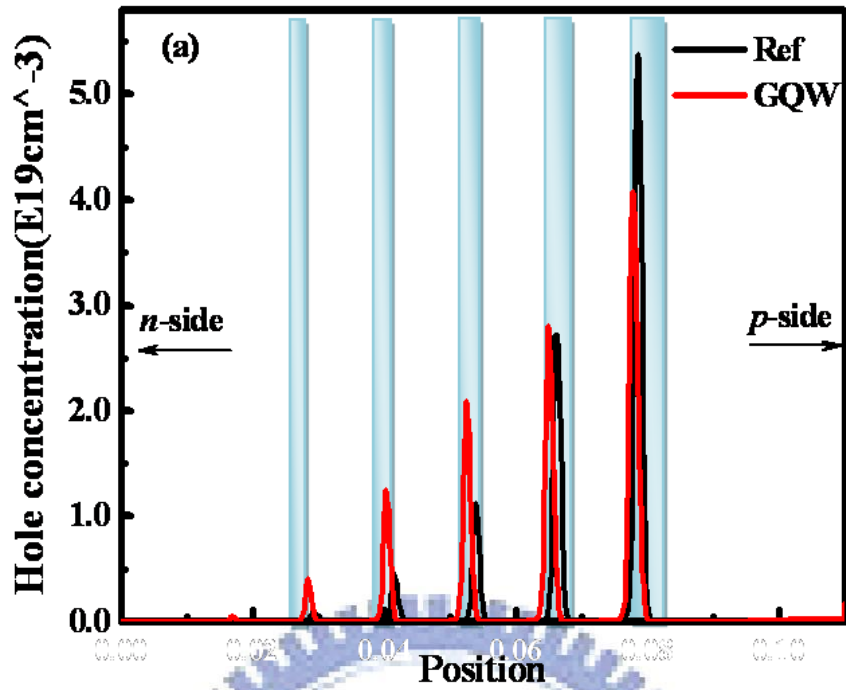


Figure 5.3.1 Simulated hole distribution in reference and GQW LEDs

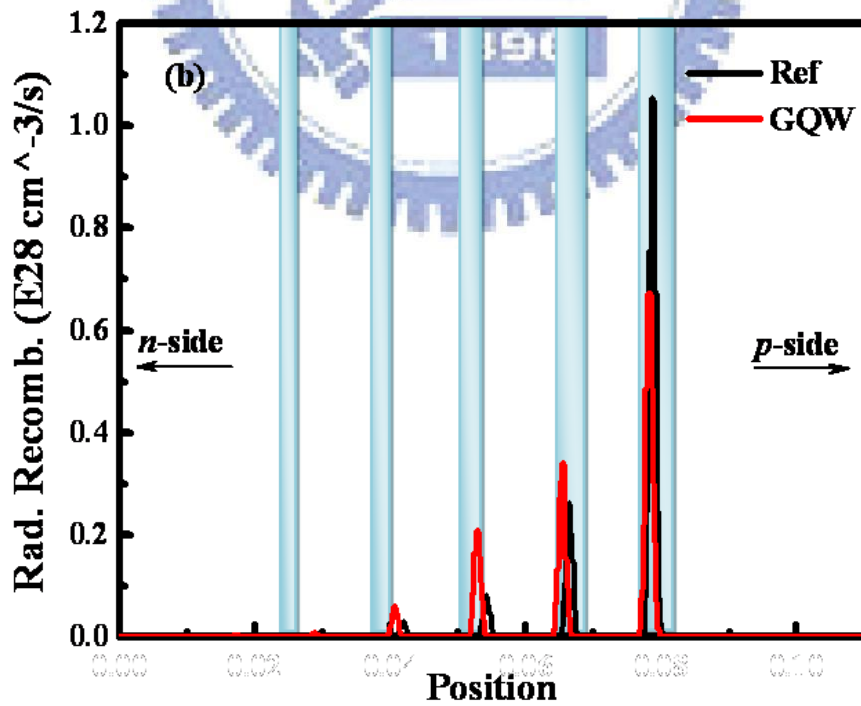


Figure 5.3.2 Simulated radiative recombination distribution

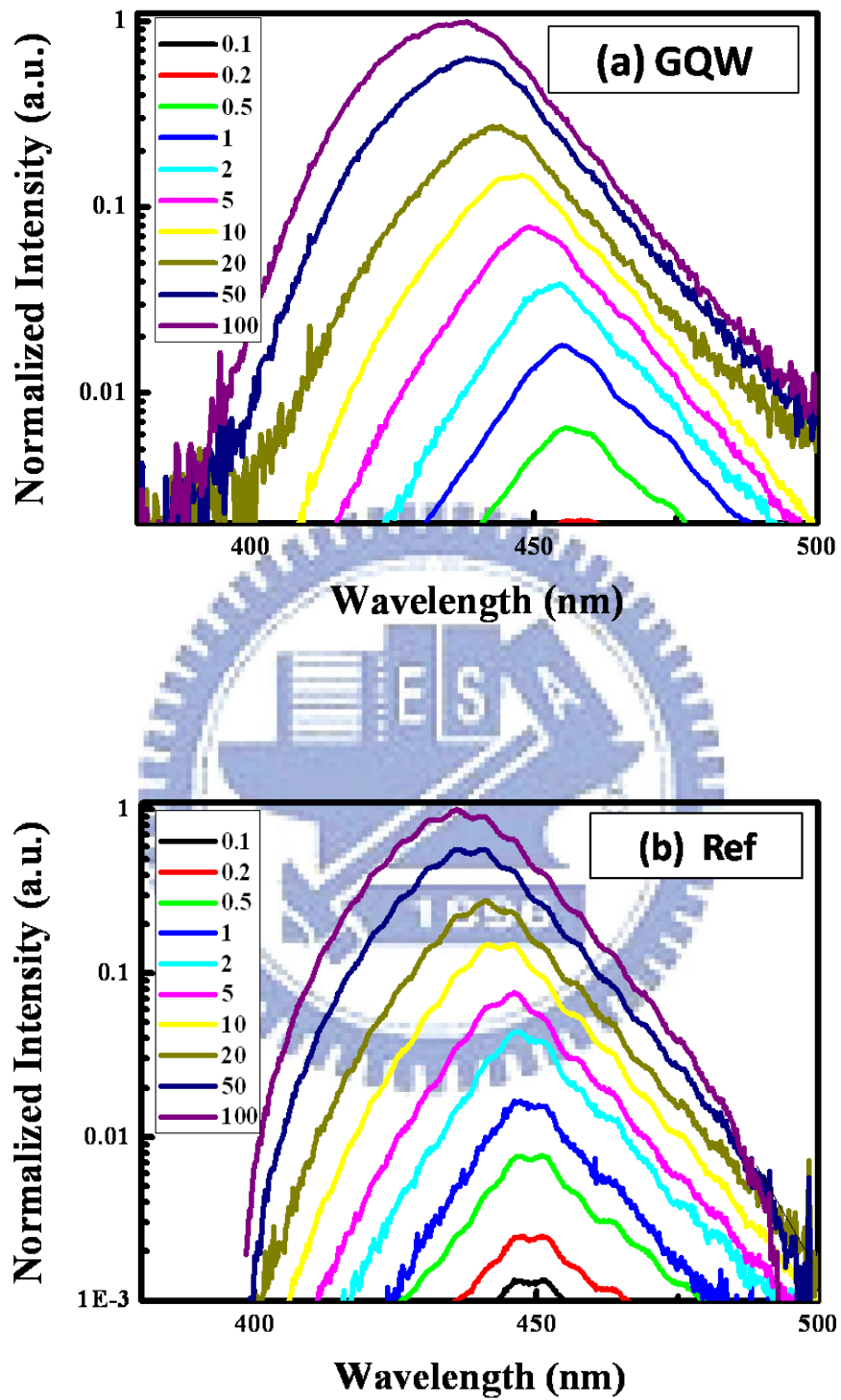


Figure 5.4.1 Current-dependent electroluminescence spectra of (a) GQW and (b) reference LEDs.

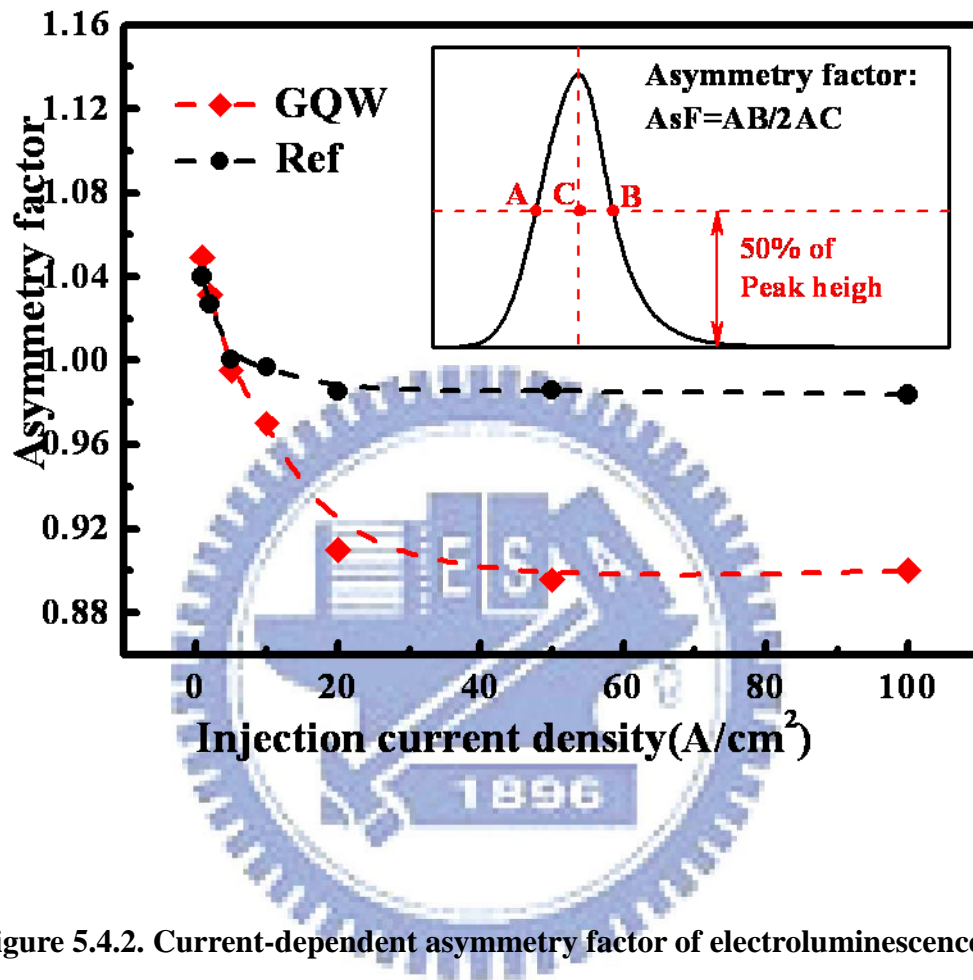


Figure 5.4.2. Current-dependent asymmetry factor of electroluminescence spectra of reference and GQW LEDs.

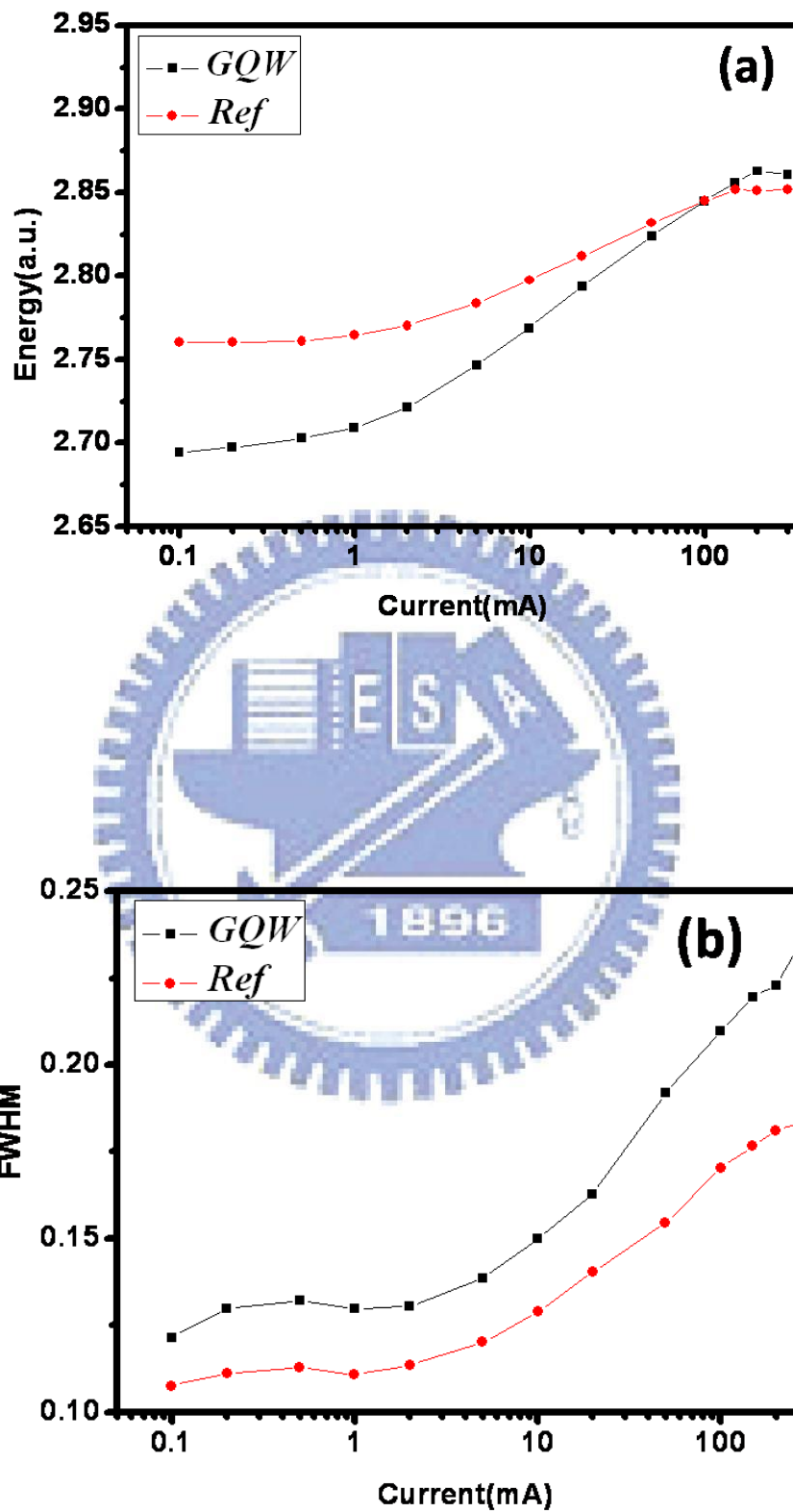


Figure 5.4.3 Current dependent emission energy and FWHM in reference and GQW LEDs

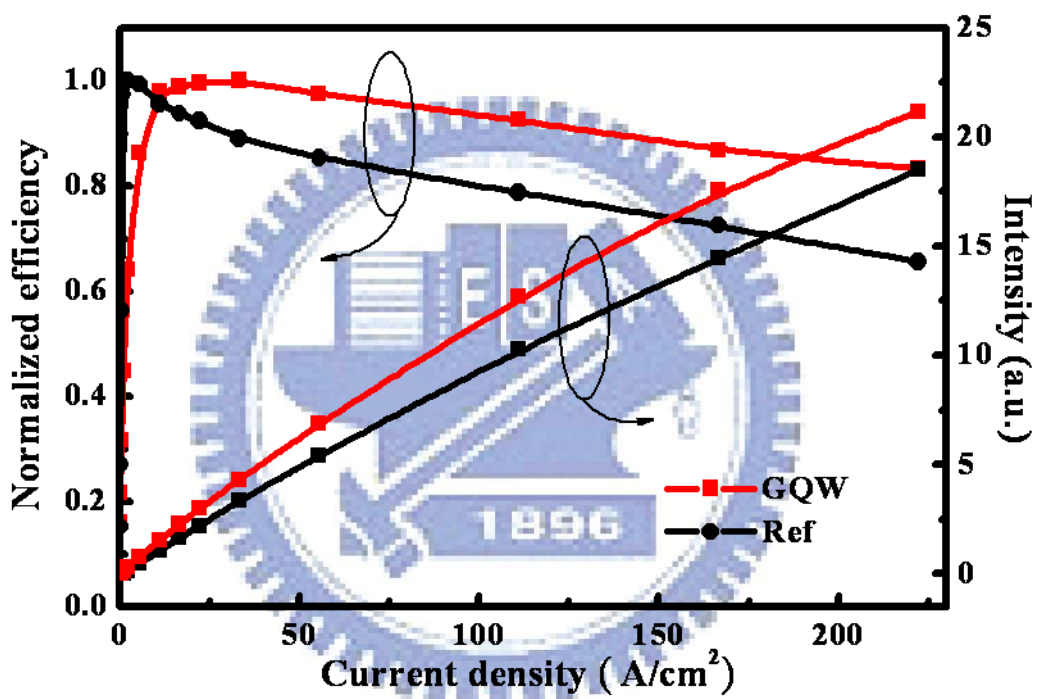
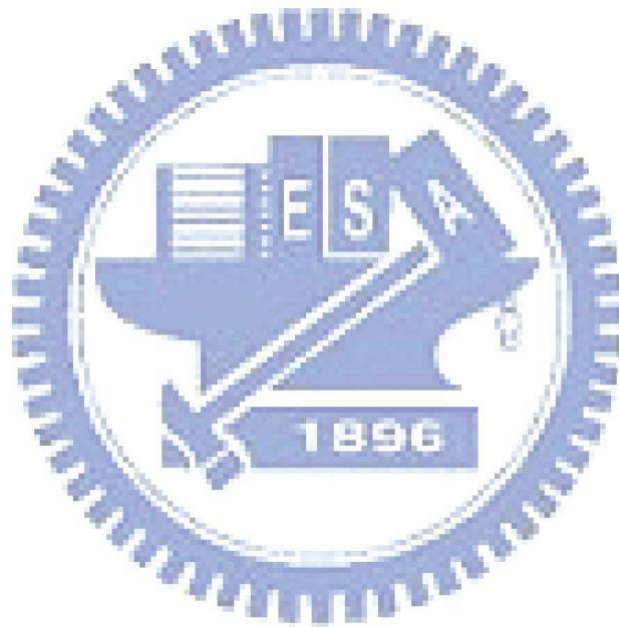


Figure 5.5.1. Comparison of normalized electroluminescence efficiency and L-I curves

Chapter 6 Conclusion

In first part, we have compared LEDs with LT-GaN, InGa/GaN and without prestrain layer. The LED with LT-GaN prestrain layer shows a great improvement in outpower and efficiency from the LED with InGa/GaN prestrain layer at high carrier density. The use of LT-GaN results in a very little blue shift of emission, less band filling effect, and reduce efficiency droop at high carrier density, compared to the reference and InGaN/GaN prestrain LEDs. These results indicate that low temperature growth GaN prestrain layer facilitate the suppression of the strain and In inhomogeneous distribution. Further, we have demonstrated relatively low efficiency droop in InGaN/GaN LEDs by graded quantum well structure as compared with the normal LEDs. The EQE is nearly retained in GQW LEDs even at a high forward current density of 244 A/cm² (only 17 % droop), whereas c-plane LEDs exhibit as high as 36% efficiency droop under the same injection current density. The light output power was also enhanced by 36% at 22 A/cm² due to more quantum well be used. The APSYS simulations indicate that superior hole distribution can be achieved in the GQW designed MQWs, in which the well-thickness increases along [0001] direction. It might be attributed to the longer radiative recombination lifetime in the wider well nearest to *p*-type layer. Moreover, by analyzing the EL spectra in detail, the additional emission from the narrower wells were demonstrated. This indicates that

more carriers distribute in the following wells, which agrees well with the simulated results. As a result, the efficiency droop behavior was alleviated from 54% in LED without any structure modified to 17% in LED with LT-GaN prestrain layer and graded quantum well. In addition, This work implies that with suitable active region design, carrier transportation behavior could be modified, which is very useful for alleviating efficiency droop.



Reference

- [1] S. Nakamura, M. Senoh, N. Isawa, and S. Nagahama, Japan Journal of Applied Physics 34,L797 (1995)
- [2] S. Nakamura, T. Mukai, and M. Senoh, Applied Physics Letter 64, 1687 (1994)
- [3] S. Nakamura, M. Senoh, S. Nagahama, N. Iwasa, T. Yamada, T. Matsushita, Y. Sugimoto, and H. Kiyoku, Applied Physics Letter 70, 868 (1997)
- [4] S. Nakamura, Science 281, 956 (1998)
- [5] Y.Arakawa, IEEE Journal of Selected Topics in Quantum Electronics 8, 823 (2002)
- [6] H. Morkoc, Nitride Semiconductors and Devices (Springer Verlag, Heidelberg), 1999
- [7] S. N. Mohammad, and H. Morkoc, Progress in Quantum Electronics 20, 361, (1996)
- [8] F. Bernardini and V. Fiorentini, Physica Status Solidi B 216, 391 (1999)
- [9] A. Hangleiter, J. S. Im, H. Kollmer, S. Heppel, J. Off, and F. Scholz, MRS Internet Journal of Nitride Semiconductor Research 3, 15 (1998)
- [10] H. Amano, N. Sawaki, I. Akasaki, and Y. Toyoda, Applied Physics Letter 48, 353(1986)
- [11] S. Nakamura, Japan Journal of Applied Physics 30, L1705 (1991)

- [12] S. Nakamura, T. Mukai, M. Senoh, S. Nagahama, and N. Iwasa, *Journal of Applied Physics* 74, 3911 (1993)
- [13] H. Amano, N. Sawaki, I. Akasaki, and Y. Toyoda, *Applied Physics Letter* 48, 353 (1986)
- [14] H. Amano, N. Sawaki, I. Akasaki, and Y. Toyoda, *Japan Journal of Applied Physics* 28,L2112 (1989)
- [15] S. Nakamura, S. Iwasa, M. Senoh, US patent 5306662
- [16] K. J. Vampola, M. Iza, S. Keller, S. P. DenBaars, and S. Nakamura, *Appl. Phys. Lett.* 94, 061116 (2009)
- [17] Y. C. Shen, G. O. Muller, S. Watanabe, N. F. Gardner, A. Munkholm, and M. R. Krames, *Appl. Phys. Lett.* 91, 141101 (2007)
- [18] Y. Yang, X. A. Cao, and C. Yan, *IEEE Transactions On Electron Devices* 55, 1771 (2008).
- [19] B. Monemar and B. E. Sernelius, *Appl. Phys. Lett.* 91, 181103 2007 .
- [20] F. Bernardini, V. Fiorentini, D. Vanderbilt, *Phys. Rev. B* 56 (1997) R10024.
- [21] O. Ambacher, B. Foutz, J. Smart, J.R. Shealy, N.G.Weimann, K. Chu, M. Murphy, A.J. Sierakowski, W.J. Schaff, L.F. Eastman, R. Dimitrov, A. Mitchell, M. Stutzmann, *J. Appl. Phys.* 87 (2000) 334.
- [22] M. Leroux, N. Grandjean, M. La. ugt, J. Massies, B. Gil, P. Lef!ebvre, P.

- Bigenwald, Phys. Rev. B 58 (1998) R13371.
- [23] S.F. Chichibu, A.C. Abare, M.P. Mack, M.S. Minsky, T. Deguchi, D. Cohen, P. Kozodoy, S.B. Fleischer, S. Keller, J.S. Speck, J.E. Bowers, E. Hu, U.K. Mishra, L.A. Coldren, S.P. DenBaars, K. Wada, T. Sota, S. Nakamura, Mater. Sci. Eng. B 59 (1999) 298.
- [24] N.A. Shapiro, Y. Kim, H. Feick, E.R. Weber, P. Perlin, J.W. Yang, I. Kasaki, H. Amano, Phys. Rev. B 62 (2000) R16318.
- [25] P. Lefebvre, A. Morel, M. Gallart, T. Taliercio, J. Allègre, B. Gil, H. Mathieu, B. Damilano, N. Grandjean, J. Massies, Appl. Phys. Lett. 78 (2001) 1252.
- [26] B. Gil, O. Briot, R.-L. Aulombard, Phys. Rev. B 52 (1995)
- [27] H. Lahrleche, M. Leroux, M. Laugt, M. Vaille, B. Beaumont, P. Gibart, J. Appl. Phys. 87 (2000) 577.
- [28] M. Leroux, H. Lahrleche, F. Semond, M. Laugt, E. Feltin, N. Schnell, B. Beaumont, P. Gibart, J. Massies, Mater. Sci.
- [29] S. Chichibu, T. Azuhata, T. Sota, and S. Nakamura, Appl. Phys. Lett. 69, 4188 (1996)
- [30] I. Ho and G. B. Stringfellow, Appl. Phys. Lett. 69, 2701 (1996)
- [31] P. Waltereit et al., J. Cryst. Growth 437, 227 (2001).
- [32] S. F. Chichibu, T. Onuma, T. Aoyama, K. Nakajima, P. Ahmet, T. Chikyow, T.

- Sota, S. P. DenBaars, S. Nakamura, T. Kitamura, Y. Ishida and H. Okumura : J. Vac. Sci. & Technol. B 21, 1856 (2003)
- [33] C. H Jang, J. K Sheu, C. M. Tsai, S. J Chang, Member, IEEE. 46, (2010)
- [34] M. H. Kim, M. F. Schubert, Q. Dai, J. K. Kim, E. F. Schubert, J. Piprek, Y. Park, Appl. Phys, Lett. 91, 183507 (2007).
- [35] K. J. Vampola, M. Iza, S. Keller, S. P. DenBaars, and S. Nakamura, Appl. Phys, Lett. 94, 061116 (2009)
- [36] K. Ding, Y. P. Zeng, X. C. Wei, Z. C. Li, J. X. Wang, H. X. Lu, P. P. Cong, X. Y. Yi, G. H. Wang, J. M. Li, Appl Phys B, 97, 465–468 (2009).
- [37] C. H. Wang, J. R. Chen, C. H. Chiu, H. C. Kuo, Y. L. Li, T. C. Lu, and S. C. Wang, IEEE Photon. Technol. Lett. 22, 236 (2010).
- [38] A. David and M. J. Grundmann, Appl. Phys, Lett. 96, 103504 (2010).
- [39] B. Monemar and B. E. Sernelius, Appl. Phys. Lett. 91, 181103 (2007).
- [40] M. F. Schubert, J. Xu, J. K. Kim, E. F. Schubert, M. H. Kim, S. Yoon, S. M. Lee, C. Sone, T. Sakong, and Y. Park, Appl. Phys. Lett. 93, 041102 (2008).
- [41] Y. K. Kuo, J. Y. Chang, M. C. Tsai, and S. H. Yen, Appl. Phys. Lett. 95, 011116 (2009).
- [42] R. A. Arif, Y. K. Ee, and N. Tansu, Appl. Phys. Lett. 91, 091110 (2007).
- [43] S. C. Ling, T. C. Lu, S. P. Chang, J. R. Chen, H. C. Kuo, and S. C. Wang, Appl.

Phys. Lett. 96, 231101 (2010).

[44] J. Xie, X. Ni, Q. Fan, R. Shimada, Ü. Özgür, and H. Morkoç, Appl. Phys. Lett. 93, 121107 (2008).

[45] I. V. Rozhansky and D. A. Zakheim, Phys. Status Solidi A 204, 227 (2007)

[46] M. H. Kim, M. F. Schubert, Q. Dai, J. K. Kim, E. F. Schubert, J. Piprek, and Y.

[47] F. Bernardini, V. Fiorentini, and D. Vanderbilt, Phys. Rev. B 56, R10024 (1997)

[48] T. Takeuchi, S. Sota, M. Katsuragawa, M. Komori, H. Takeuchi, H. Amano, and I. Akasaki, Jpn. J. Appl. Phys., Part 2 36, L382 (1997)

[49] Y. H. Cho, G. H. Gainer, A. J. Fischer, J. J. Song, S. Keller, U. K. Mishra, and S. P. Denbaars, ““S-shaped” temperature-dependent emission shift and carrier dynamics in InGaN/GaN multiple quantum wells,” Appl. Phys. Lett., vol. 73, no. 10, p. 1370, Sep. 1998.

[50] C. A. Tan, R. F. Karliceck, Jr., M. Schurman, A. Osinsky, V. Merai, Y. Li, I. Eliashevich, M. G. Brown, J. Nering, I. Fergerson, and R. Stall, “Phase separation in InGaN/GaN multiple quantum wells and its relation to brightness of blue and green LEDs,” J. Cryst. Growth, vol. 195, p. 397, Dec. 1998.

[51] IEEE JOURNAL OF QUANTUM ELECTRONICS, VOL. 46, NO. 3, MARCH 2010 Cheng-Huang Kuo, Y. K. Fu, G. C. Chi, and Shou-Jinn Chang, Member, IEEE

- [52] M. F. Schubert, J. Xu, J. K. Kim, E. F. Schubert, M. H. Kim, S. Yoon, S. M. Lee, C. Sone, T. Sakong, and Y. Park, *Appl. Phys. Lett.* 93, 041102 (2008).
- [53] Y. K. Kuo, J. Y. Chang, M. C. Tsai, and S. H. Yen, *Appl. Phys. Lett.* 95, 011116 (2009).
- [54] R. A. Arif, Y. K. Ee, and N. Tansu, *Appl. Phys. Lett.* 91, 091110 (2007).
- [55] S. C. Ling, T. C. Lu, S. P. Chang, J. R. Chen, H. C. Kuo, and S. C. Wang, *Appl. Phys. Lett.* 96, 231101 (2010).
- [56] J. Xie, X. Ni, Q. Fan, R. Shimada, Ü . Ö zgür, and H. Morkoç, *Appl. Phys. Lett.* 93, 121107 (2008).
- [57] X. Ni, Q. Fan, R. Shimada, Ü . Ö zgür, and H. Morkoç, *Appl. Phys. Lett.* 93, 171113 (2008).
- [58] I. Vurgaftman and J. R. Meyer, *J. Appl. Phys.* 94, 3675 (2003).
- [59] A. David, M. J. Grundmann, J. F. Kaeding, N. F. Gardner, T. G. Mihopoulos, and M. R. Krames, *Appl. Phys. Lett.* 92, 053502 (2008).